



OPEN ACCESS

EDITED BY

Delphine Thibault,
Aix-Marseille Université, France

REVIEWED BY

Zafrir Kuplik,
Tel-Aviv University, Israel
Dhugal John Lindsay,
Japan Agency for Marine-Earth Science and
Technology (JAMSTEC), Japan

*CORRESPONDENCE

Aino Hosia
aino.hosia@uib.no

RECEIVED 22 April 2024

ACCEPTED 02 September 2024

PUBLISHED 15 October 2024

CITATION

Hosia A, Martell L, Mańko MK, Haddock SHD, Haberlin D and Mapstone GM (2024) Unexpected diversity and novel lineages in the cosmopolitan genus *Nanomia* (Cnidaria: Siphonophorae: Physonectae). *Front. Mar. Sci.* 11:1421514. doi: 10.3389/fmars.2024.1421514

COPYRIGHT

© 2024 Hosia, Martell, Mańko, Haddock, Haberlin and Mapstone. This is an open-access article distributed under the terms of the Creative Commons Attribution License (CC BY). The use, distribution or reproduction in other forums is permitted, provided the original author(s) and the copyright owner(s) are credited and that the original publication in this journal is cited, in accordance with accepted academic practice. No use, distribution or reproduction is permitted which does not comply with these terms.

Unexpected diversity and novel lineages in the cosmopolitan genus *Nanomia* (Cnidaria: Siphonophorae: Physonectae)

Aino Hosia^{1*}, Luis Martell¹, Maciej K. Mańko², Steven H. D. Haddock³, Damien Haberlin⁴ and Gillian M. Mapstone⁵

¹Department of Natural History, University Museum of Bergen, University of Bergen, Bergen, Norway,

²Laboratory of Plankton Biology, Department of Marine Biology and Biotechnology, University of Gdańsk, Gdynia, Poland, ³MBARI, Monterey Bay Aquarium Research Institute, Moss Landing, CA, United States,

⁴MaREI – Science Foundation Ireland Research Centre for Energy, Climate and Marine, Environmental Research Institute, University College Cork, Cork, Ireland, ⁵Department of Life Sciences, The Natural History Museum, London, United Kingdom

Integrated use of molecular and morphological methods reveals unexpected diversity in the cosmopolitan siphonophore genus *Nanomia*. Species delimitation analyses based on COI and 16S sequences suggest up to three distinct lineages in addition to the previously accepted *Nanomia bijuga* (Delle Chiaje, 1844) and *N. cara* A. Agassiz, 1865. Here, we describe the North Pacific *Nanomia septata* sp. n., previously confused with both *N. cara* and *N. bijuga*, and provide improved morphological characters for the identification of these three *Nanomia* species. Phylogenetic analyses suggest two additional, hitherto undescribed clades from Japanese and Chinese waters, respectively, but the lack of morphological material prevents describing these putative species. The geographic distribution of molecularly and/or morphologically verified observations confirm a warm circumglobal distribution for *N. bijuga* and a boreal North Atlantic distribution for *N. cara*. Interestingly, four distinct lineages occur in the North Pacific, sometimes in close proximity. These contrasting patterns of distribution raise questions about pelagic speciation processes.

Nanomia septata sp. n.: urn:lsid:zoobank.org:act:DAF15EA3-AFEA-4AE8-

984F-BDFBCFE7E514

urn:lsid:zoobank.org:pub:478049FC-F672-4D34-ABAE-CF4345EC64D7

KEYWORDS

siphonophores, speciation, holoplankton, DNA barcoding, COI, 16S

1 Introduction

Widespread or cosmopolitan distributions have been assumed to be commonplace for planktonic organisms, including siphonophores, due to the apparent uniformity of their pelagic environment and lack of physical barriers to dispersal (but see [Johnson et al., 2022](#)). However, the emergence of molecular methods has revealed that many morphologically described planktonic species in fact consist of clusters of cryptic or pseudocryptic species ([Norris, 2000](#)), also for siphonophores ([Pontin and Cruickshank, 2012](#); [Grossmann et al., 2013, 2014](#); [Panasiuk et al., 2019](#)). Significant genetic divergence is seen between the Atlantic and Pacific populations of siphonophores ([Dunn et al., 2005](#)), and several species show large inter-geographic and intra-specific genetic distances, indicative of potential cryptic species ([Grossmann et al., 2014](#)). Traditional morphology-based taxonomy may thus be significantly underestimating pelagic diversity, as it does not account for this cryptic diversity ([Norris, 2000](#)). Unravelling the taxonomy of cryptic species groups requires the integrated use of molecular methods and careful morphological examination.

Agalmatid physonect siphonophores of the genus *Nanomia* are a common globally distributed component of gelatinous plankton communities ([Mapstone, 2014](#)), at times forming dense swarms or blooms ([Browne et al., 1898](#); [Rogers et al., 1978](#); [Mills, 1995](#); [Knutsen et al., 2018](#)). The genus *Nanomia* currently comprises two species: *N. cara* A. [Agassiz, 1865](#) and *N. bijuga* ([Delle Chiaje, 1844](#)). While both species are frequently reported from surveys, there has been some confusion regarding their morphological identification and geographic distributions. It is likely that *Nanomia* specimens are often misidentified or assigned to a species primarily based on the observation locality and the presumed distributions of the two accepted species, rather than as a result of a proper morphological identification. This is partly because it can be challenging to identify specimens using existing identification literature (e.g., [Totton, 1965](#); [Kirkpatrick and Pugh, 1984](#); [Pugh, 1999](#); [Bouillon et al., 2004](#); [Mapstone, 2009](#)).

The respective type localities of *N. cara* A. [Agassiz, 1865](#) and *N. bijuga* ([Delle Chiaje, 1844](#)) are Nahant, Massachusetts, in the NW Atlantic and the Gulf of Naples in the Mediterranean. Both species have been historically known under a variety of synonyms (see e.g. [Schuchert, 2024](#); [Totton, 1965](#); [Mapstone, 2009](#)) and were not reassigned to the same genus until about a century after their description, by [Totton, 1954](#). To add to the confusion around *Nanomia* identification and nomenclature, [Sars \(1846\)](#) described and made detailed illustrations of a new species, *Agalmopsis elegans*, observed in Florø, Norway. Unfortunately, this was a compound species, depicting the nectophores of *Nanomia cara* together with the tricornuate tentilla of *Agalma elegans* ([Sars, 1846](#), Pl. 5 & 6). The currently accepted view assumes a cosmopolitan distribution between 55° N and 59° S for *N. bijuga* and a more restricted North Atlantic and Arctic (40–64° N) distribution for *N. cara* ([Totton, 1965](#); [Pugh, 1999](#); [Mapstone, 2014](#)).

Like other siphonophores, *Nanomia* spp. are colonial animals consisting of physiologically integrated, specialized zooids

organized in a species-specific pattern. When collected by plankton nets, the colonies most often disassociate, with various detached zooids and more or less bare stems bearing the pneumatophore observed in the sample. While counting the pneumatophores can provide an estimate of the number of physonect colonies in the sample, nectophores are the zooid most commonly used for species identification. In addition to often being the most conspicuous of the detached zooids, nectophores have several characters including general shape, pigmentation, and the pattern of canals and ridges that can be used to infer species.

According to taxonomic literature, the key character used to separate the two *Nanomia* species is the plane in which their nectophores are flattened. Depending on the terminology used, *N. bijuga* nectophores are described as flattened from stem to ostial side, in the vertical plane ([Totton, 1965](#)) or along the proximal-distal axis ([Mapstone, 2009](#)), while *N. cara* nectophores are flattened in the horizontal plane ([Totton, 1965](#)) or along the upper-lower axis ([Mapstone, 2009](#)) in a manner typical of many other physonects. In his comparison of the two species, [Totton \(1954\)](#) also mentions the presence of an oil droplet at the base of the palpons as being characteristic of *N. cara*, but such oil droplets have since also been shown to occur in *N. bijuga* from the Pacific ([Mapstone, 2009](#); [Church et al., 2015](#)). [Totton \(1954\)](#) further describes some differences in pigmentation, and *N. cara* colonies have been suggested to generally grow to a larger size than *N. bijuga* ([Mapstone, 2009](#)). However, the latter two characters are likely variable and thus of limited value for identification and can also be impossible to infer from detached or preserved nectophores. [Totton \(1965\)](#) concluded that while the two *Nanomia* species can be told apart by their nectophores, to what extent they differ in other respects has not been determined, and the literature published since then has done little to clarify this situation.

While separating the two species based on their nectophore morphology sounds straightforward, it has proven to be challenging in practice. The two extremes of nectophore morphology, as illustrated for *N. cara* by [Totton \(1954\)](#) and *N. bijuga* by [Kawamura \(1911\)](#), are easy enough to tell apart, but samples often contain nectophores of intermediate habitus that are not easily assigned to either species. The taxonomic literature also illustrates a continuum of nectophore shapes, with the Pacific *Nanomia* in particular having an intermediate form ([Figure 1](#)). To further complicate identification, net caught specimens have often suffered damage during sampling, and nectophores fixed in formalin undergo varying stages of contraction and tend to lose their coloration as well as their life-like shape, since the mesogloea may become very soft.

Subsequently, the identification of *Nanomia* can pose difficulties. *Nanomia* is ubiquitous throughout NE Atlantic waters, from around Great Britain and North Sea in the south, along the entire Norwegian coast including in the fjords, and all the way up to the Arctic region in Atlantic waters ([Kirkpatrick and Pugh, 1984](#); [Hosia and Båmstedt, 2008](#); [Knutsen et al., 2018](#)). While literature suggests that it is *N. cara* that occurs in NE Atlantic waters, nectophores with intermediate morphology are often observed in Norwegian waters, making identification doubtful. Further confusion regarding the species identity of NE Atlantic

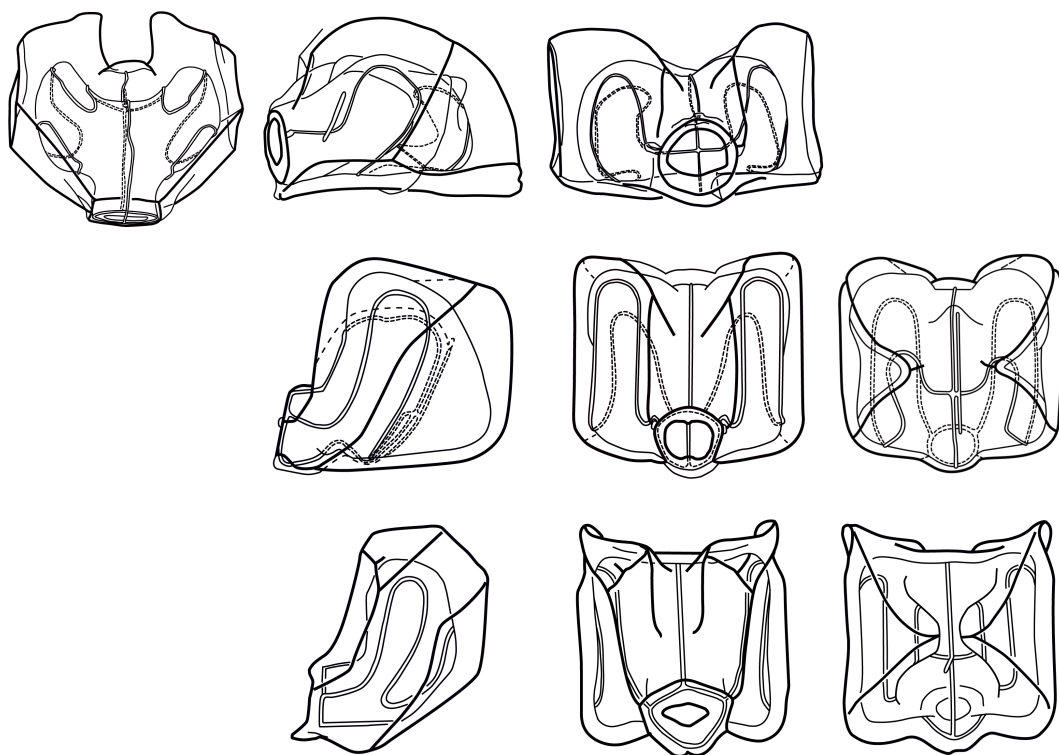


FIGURE 1

Range of *Nanomia* nectophore shapes. Upper, lateral, distal and proximal views (left to right). From top to bottom: NE Atlantic *N. cara* (Totton, 1954), NE Pacific *N. septata* sp. n (Mapstone, 2009, as *N. bijuga*), and NW Pacific *N. bijuga* (Kawamura, 1911). Reproduced with permission of The Trustees of the Natural History Museum, London; Canadian Science Publishing; and the Zoological Society of Japan, respectively. These images are not covered by the terms of the Creative Commons license of this publication. For permission to reuse, please contact the relevant rights holder.

Nanomia has recently been added by three investigations from Ireland, which have suggested that the species collected in Irish waters is *N. bijuga*, based on 18S molecular (Baxter et al., 2012) and morphological (Haberlin et al., 2016, 2019) characters. Baxter et al. (2012) go as far as to suggest that the species occurring in colder, temperate waters of the North Atlantic should generally be considered *N. bijuga*, rather than *N. cara*, as has been previously assumed. Similarly, *Nanomia* from the northeast Pacific have historically been referred to as both *N. cara* and, more recently, *N. bijuga* (see e.g. Mackie, 1964; Mapstone, 2009).

This study began with a need to assign *Nanomia* specimens occurring in NE Atlantic waters, and Norway in particular, to the correct species. To resolve this issue, we have applied integrated molecular and morphological methods to study the diversity in the genus *Nanomia*. *Nanomia* nectophores with varying size and morphology were collected for examination and genetic barcoding from several locations in the NE Atlantic, the Mediterranean, and the Pacific Ocean. Collected specimens were sequenced for cytochrome oxidase I (COI) and 16S ribosomal RNA mitochondrial markers, both known to be suited for DNA barcoding and species delimitation in hydrozoans (Ortman et al., 2010; Zheng et al., 2014; Lindsay et al., 2015). Specimens from various locations, as well as available material from natural history collections, were examined in detail to uncover hitherto overlooked morphological differences. Phylogenetic analyses were performed on the obtained 16S and COI sequences together with *Nanomia*

sequences received from collaborators or mined from GenBank and BOLD repositories, as well as other agalmatid sequences.

2 Materials and methods

2.1 Sampling

Nanomia colonies and/or nectophores were sampled during several field campaigns using various plankton nets, by snorkeling, blue-water scuba diving, or remotely operated vehicles at several locations in the North Atlantic, the Arctic, the Mediterranean, the North and Central Pacific, and the Gulf of California. Additional nectophores and colonies were contributed by collaborators (Supplementary Table S1). While the exact procedure varied between sampling events, specimens for morphological examination were generally fixed in ~4% borax-buffered formalin in sea water, while nectophores for molecular work were photographically documented prior to being individually flash frozen or preserved in >96% ethanol.

2.2 DNA extraction, amplification and sequencing

Tissue fragments were taken from frozen or ethanol fixed specimens selected for molecular work. When dealing with loose

nectophores, only one nectophore per net sample was chosen to avoid accidentally sequencing several nectophores from a single colony. DNA extraction and sequencing for both cytochrome oxidase I (COI) and 16S ribosomal RNA mitochondrial markers were performed either in-house at the University of Bergen or at the Monterey Bay Aquarium Research Institute (MBARI), or at the Canadian Centre for DNA Barcoding (CCDB) in Guelph. For the work at CCDB, we submitted tissue samples and data according to the routines in BOLD (www.boldsystems.org). CCDB used their tissue lysis protocol and applied the following primer pairs for PCR amplification and sequencing: SHA/SHB for 16S ([Cunningham and Buss, 1993](#)), and either C_LepFolF/C_LepFolR ([Hernández-Triana et al., 2014](#)) or COF/CoR (Schuchert, unpublished, sequence available at www.boldsystems.org/index.php/Public_Primer_PrimerSearch) for COI. In Bergen, the Qiagen DNeasy Blood and Tissue Kit protocol was used for extraction. Partial sequences of COI (ca. 660 bp) and 16S (ca. 560 bp) were amplified using the primer-pairs LCO/HCO ([Folmer et al., 1994](#)) and SHA/SHB ([Cunningham and Buss, 1993](#)), respectively. PCR conditions for amplification of COI were initial denaturation at 94°C for 5 min, 5 cycles of 94°C for 45 s, annealing at 45°C for 30 s, and extension at 72°C for 1 min, 31 cycles of 94°C for 45 s, annealing at 50°C for 30 s, and extension at 72°C for 1 min, and final extension at 72°C for 10 min. PCR conditions for amplification of 16S were initial denaturation at 94°C for 5 min, 40 cycles of 94°C for 30 s, annealing at 50°C for 30 s, and extension at 72°C for 1 min, and final extension at 72°C for 10 min. Successful PCR products were purified with ExoSAP-IT (Thermo Fisher Scientific). Sequence reactions using Big Dye 3.1 and the PCR primers were run on an ABI 3730XL DNA Analyser (Applied Biosystems). Assembly of forward and reverse sequences was performed with Geneious (version 11.1.5) ([Kearse et al., 2012](#)). All sequences of *Nanomia* spp. available at Barcode of Life Datasystems (BOLD) and GenBank were downloaded and included in further analyses, together with the sequences generated in this study, by [Knutzen et al. \(2018\)](#), or received from collaborators ([Supplementary Table S1](#)).

2.3 Sequence alignment, phylogenetic analyses, and molecular species delimitation

Sequences were visualized and edited in Geneious v.11.1.5 ([Kearse et al., 2012](#)), and their identity was verified by BLAST searches against the GenBank nucleotide database to check for contamination. GenBank sequence KF977400 was discarded at this point due to misidentification (while labelled as *Nanomia bijuga*, the sequence in fact belongs to *Diphyes* sp.). GenBank sequences KF962059 and KF962394 (both labelled as *Agalma elegans*) and KF977379 (labelled as *Euchaeta concinna*) were found to be virtually identical to GenBank sequences KF977305, KF977401, and KF977402 assigned to *N. bijuga*; however, only sequences originally identified as *Nanomia* were included in the analyses. Sequences belonging to the phyonect genera *Agalma*, *Athorybia*, *Halistemma*, *Marrus*, *Apolemia*, and *Physophora* were selected as outgroups for the analysis based on their close phylogenetic position in relation to

Nanomia, following [Munro et al. \(2018\)](#). An alignment was created independently for each of the markers using MUSCLE ([Edgar, 2004](#)) as implemented in MEGA v.10.2.5 ([Kumar et al., 2018](#)). The alignments were trimmed to a position at which all the sequences had nucleotides. For COI, nucleotide reads were translated to amino acids to check for potential stop codons. After trimming and editing, a total of 85 COI (520 bp) and 57 16S (536 bp) high quality sequences were included in the phylogenetic and species delimitation analyses. All new sequences have been deposited in GenBank and/or BOLD Systems ([Supplementary Table S1](#)).

Gene trees were estimated independently for the above 16S and COI alignments. The sequences were analyzed using a phylogenetic approach based on (a) maximum likelihood (ML) optimality criterion in RaxML v8.2.8 ([Stamatakis, 2014](#)) and (b) Bayesian inference using MrBayes v. 3.2.6 ([Ronquist et al., 2012](#)). The best-fit model for each dataset was calculated using jModelTest v. 2.1.5 ([Darriba et al., 2012](#)) with default settings and chosen using the Akaike Information Criterion (AIC). For both datasets the best-fit model was GTR+I+G. In the ML analyses, a maximum likelihood consensus tree was generated for each marker by conducting a heuristic search and bootstrapping with 500 replicates. In the Bayesian analyses four parallel Markov chain Monte Carlo (MCMC) runs were carried out for 500000 generations. Trees were sampled every 100 generations, discarding the initial 25% as burn-in.

Two methods of molecular species delimitation were applied to the genetic data: (1) Assemble species by automatic partitioning (ASAP) ([Puillandre et al., 2021](#)) and (2) Poisson Tree Processes (bPTP) ([Zhang et al., 2013](#)). Both ASAP and bPTP were applied independently to the COI and 16S datasets. Analyses were performed through <https://bioinfo.mnhn.fr/abi/public/asap/webservice> for ASAP, and <http://species.h-its.org/> for bPTP. The input files for ASAP were the trimmed alignments for each marker (with the exclusion of the outgroups), and for bPTP the rooted ML trees obtained in the phylogenetic analyses. To estimate inter- and intra-specific genetic distances based on the species hypotheses recovered in the ASAP and bPTP analysis, pairwise distances were calculated for the COI and 16S alignments using the Kimura 2-parameter model (K80) with 500 bootstrap replicates in MEGA version v. 10.2.5 ([Kumar et al., 2018](#)).

2.4 Morphology

Preserved and live specimens ([Supplementary Table S1](#)) were examined and photographed using stereomicroscopes with attached cameras. All zooids were imaged, and composite drawings were made of mature nectophores and of bracts.

3 Results

Our results indicate that the genus *Nanomia* shows significant genetic divergence beyond the two currently accepted species. Based on both molecular evidence and morphological examination of specimens representing the different genetic lineages and geographic regions, we conclude that the *Nanomia* occurring in

northeastern Pacific should be considered a separate species, *Nanomia septata* sp. n., and provide a description of the species. Observed characteristics of the examined *N. cara* and *N. bijuga* material are also given for comparison, but this should not be considered a formal re-description of these species. Improved characters for the identification of the three species are provided (**Table 1**). Our species delimitation analyses further support two additional *Nanomia* lineages recorded from Chinese and Japanese waters, respectively (**Figures 2, 3**). Unfortunately, we have not been able to examine the detailed morphology of any specimens belonging to these clades. The sequences forming the Chinese clade are mined from GenBank, while the three ectophores collected at Shimoda, Japan, were fixed in ethanol with poor photographic documentation, and used for sequencing in their entirety. These latter ectophores were *Nanomia*-like in habitus (ridges and radial canals), ~2 mm in height, and with a conspicuous red pigment spot on either side of the ostium. However, we are

currently unable to provide a more detailed description of these ectophores or the rest of the colonies.

3.1 Phylogenetic analyses and molecular species delimitation

Both ASAP and bPTP identified 5 putative species (*N. cara*, *N. bijuga*, *N. septata* sp. n., an undescribed *Nanomia* clade from Japanese waters, hereafter *Nanomia* sp.1 Japan, and another undescribed *Nanomia* clade from Chinese waters, hereafter *Nanomia* sp.2 China) in the COI dataset (**Figure 3**), corresponding to the clades identified in the Bayesian analysis with posterior probability > 0.95 and in the ML analysis with bootstrap supports of 99–100% (**Figure 3**; **Supplementary Figure S1**). In the 16S dataset (**Supplementary Figure S2**), bPTP recovered the same 5 putative species, while ASAP failed to separate between *N. bijuga* and *Nanomia* sp.1 Japan, thus suggesting 4

TABLE 1 Summary of diagnostic features separating *Nanomia* spp.

	<i>N. septata</i> sp. n.	<i>N. bijuga</i>	<i>N. cara</i>
Pneumatophore	Red apex, conspicuous longitudinal septa lines in fixed specimens. Length up to 5 mm.	Red apex, no conspicuous longitudinal septa lines. Length up to at least 2 mm.	Red apex, no conspicuous longitudinal septa lines. Length up to at least 2 mm.
Nectophore shape	Shape cuboid/flattened parallel to stem along proximal-distal axis.	Flattened parallel to stem along proximal-distal axis.	Small ectophores cuboid/flattened parallel to stem along proximal-distal axis. Larger ectophores flattened along the upper-lower axis.
Auriculate ridge	No	Yes	No
Junction of lateral and upper lateral ridges	Junction more distal, with a short incomplete continuation of upper lateral ridge.	Junction more proximal, with a long incomplete continuation of upper lateral ridge.	Junction more distal, with a very short incomplete continuation of upper lateral ridge.
Palpons	Some with internal proximal lipid droplet	Without lipid droplet	With external proximal lipid droplet

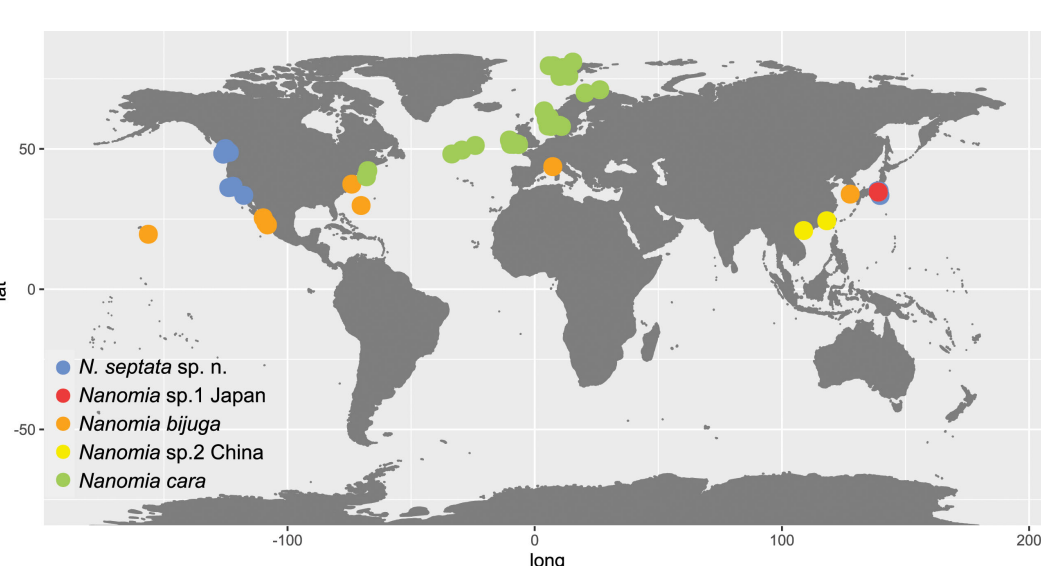


FIGURE 2
Map of *Nanomia* observations listed in **Supplementary Table S1**.

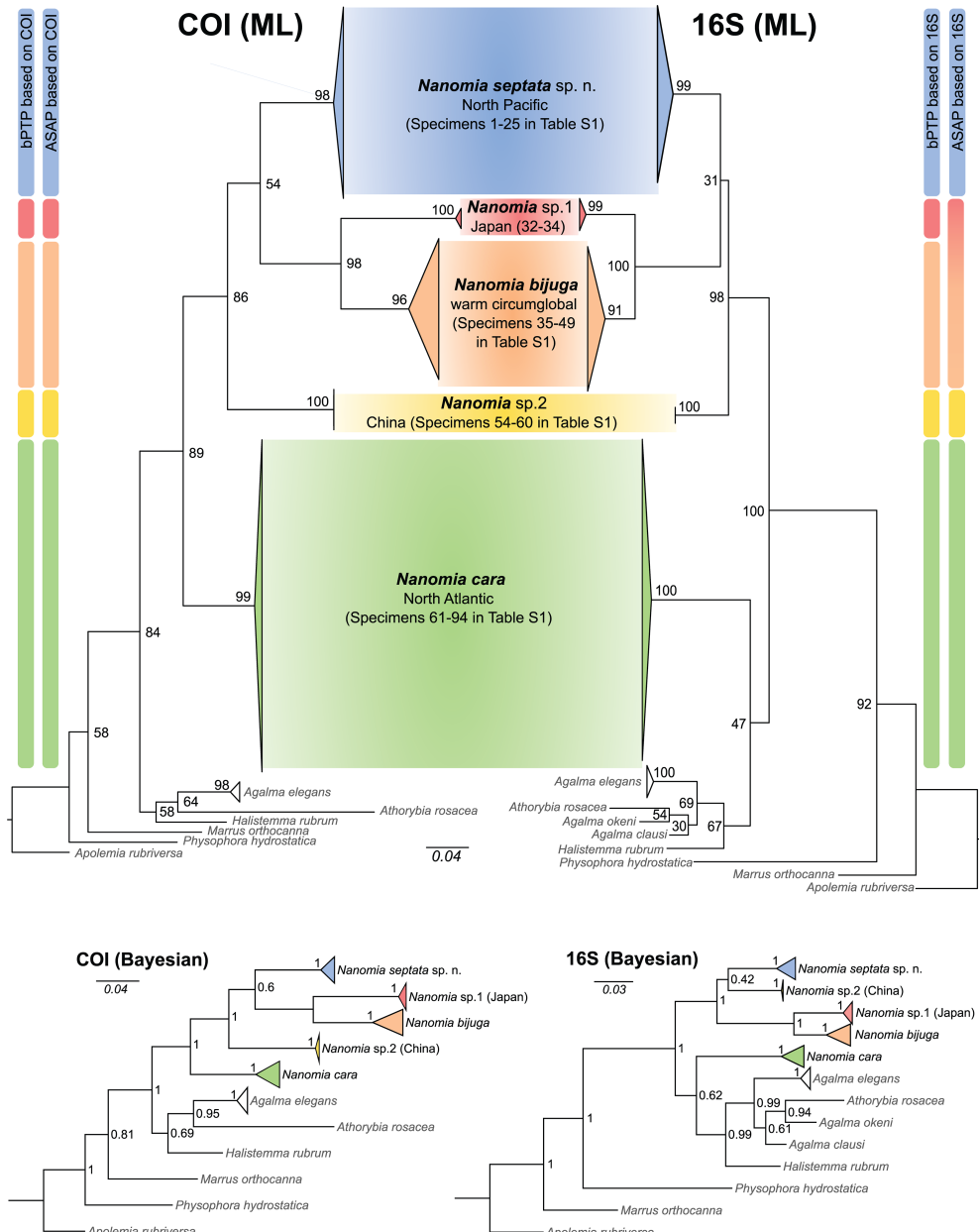


FIGURE 3

Generalized maximum likelihood phylogenies based on COI and 16S sequences (bootstrap values on nodes), putative species identified by ASAP and bPTP, and alternative topologies from Bayesian analyses (posterior probabilities on nodes).

putative species (Figure 3). The analysis of the intra- and interspecific Kimura 2-distances supports the splitting of our datasets in 5 putative species (Table 2). The mean interspecific distance (\pm SD) between *Nanomia* species was $17.7\% \pm 1.1\%$ for COI and $13.4\% \pm 2.2\%$ for 16S. The smallest interspecific distance ($15.3\% \pm 0.6\%$ for COI, $7.10\% \pm 0.2\%$ for 16S) was found between *N. bijuga* and *Nanomia* sp. 1 Japan, while the largest interspecific distance ($19.8\% \pm 0.2\%$ for COI and $16.4\% \pm 0.3\%$ for 16S) was found between *N. cara* and *Nanomia* sp. 1 Japan. *Nanomia bijuga* showed the highest intraspecific variation ($2.4\% \pm 1.2\%$ for COI, $1.2\% \pm 0.9\%$ for 16S), and geographically structured clustering could also be observed within the clade

(Supplementary Figures S1, S2). The consensus trees for both COI and 16S showed bootstrap support of $>99\%$ and posterior probabilities of 1 for all putative species clades (Figure 3). The geographical distribution of the identified clades of *Nanomia* is presented in Figure 2. Four of the putative species correspond with a distinct Barcode Index Number (BIN) in the Barcode of Life Database (BOLD): *Nanomia* sp.2 China corresponds to BIN ACH6037, *N. bijuga* to BIN AAX3682, *N. cara* to ACQ6137 and *N. septata* n.sp. to BIN ACL8638. There are no prior publicly available COI sequences for the undescribed *Nanomia* sp.1 Japan in BOLD.

TABLE 2 Summary of mean pairwise intra- and interspecific K2P distances (% \pm SD) in COI and 16S for the five putative *Nanomia* species.

		<i>N. bijuga</i>	<i>N. cara</i>	<i>N. septata</i> sp. n.	<i>Sp. n. 1</i> Japan	<i>Sp. n. 2</i> China	<i>n</i>
COI	<i>N. bijuga</i>	2.4 \pm 1.2					15
	<i>N. cara</i>	18.8 \pm 0.4	0.2 \pm 0.2				34
	<i>N. septata</i> sp. n.	17.5 \pm 0.5	17.3 \pm 0.2	0.3 \pm 0.2			20
	<i>Sp. n. 1</i> Japan	15.3 \pm 0.6	19.8 \pm 0.2	17.9 \pm 0.2	0.4 \pm 0.2		3
	<i>Sp. n. 2</i> China	19.3 \pm 0.4	16.8 \pm 0.2	15.5 \pm 0.2	19.6 \pm 0.2	0.0 \pm 0.0	5
16S	<i>N. bijuga</i>	1.2 \pm 0.9					10
	<i>N. cara</i>	15.5 \pm 0.3	0.1 \pm 0.2				21
	<i>N. septata</i> sp. n.	11.6 \pm 0.2	13.2 \pm 0.2	0.3 \pm 0.3			12
	<i>Sp. n. 1</i> Japan	7.1 \pm 0.2	16.4 \pm 0.3	11.9 \pm 0.4	0.6 \pm 0.1		3
	<i>Sp. n. 2</i> China	11.7 \pm 0.1	13.7 \pm 0.1	7.9 \pm 0.1	12.7 \pm 0.1	0.0 \pm 0.0	2

n is the number of sequences for the given species.

Shading indicates 5% intervals starting at 0 (no shading).

3.2 Account of the species examined

Genus *Nanomia* Agassiz, 1865.

Diagnosis. Monoecious Agalmatidae with colony linear; pneumatophore with red apex and an apical pore; red/orange-rust pigment spots along stem and at proximal end of gastrozooids and some other zooids; nectosome dorsal; many nectophores when mature, with incomplete upper-lateral ridges, complete lateral and vertical-lateral ridges; nectosac of nectophore with axial processes, straight upper and lower radial canals and sinuous lateral radial canals; definitive tentilla of gastrozooid tentacles unicornuate, with incomplete involucrum and single terminal filament. Male and female gonodendra characteristically in pairs on either side of the palpons, alternating sides (Totton, 1965; Dunn and Wagner, 2006). Two types of bracts, one rectangular and more prismatic, other elongate with three distinct distal cusps; often with additional ectodermal cell patches.

3.2.1 *Nanomia bijuga* (Delle Chiaje, 1844)

Material examined is specified in [Supplementary Table S1](#).

Diagnosis. Longitudinal septa in pneumatophore indistinct; nectosome with red pigment spots. Nectophores flattened along proximal-distal axis when mature, parallel to stem axis, with red spot flanking ostium on each side; axial wings bent over onto proximal side, partly enclosing stem; shallow axial groove between wing bases in mature nectophores; auriculate ridge between upper-lateral ridge and lateral ridge; thrust block small and insignificant in all nectophores. Palpon without proximal lipid droplet.

Barcode Index Number (BIN) in BOLD: AAX3682.

Description

Pneumatophore: 2.0 mm long (in largest preserved specimen), with red pigmented apex ([Figure 4](#)); some pneumatophores with faint longitudinal and transverse lines on surface, but no thick septal lines. Gas gland in lower third of pneumatophore.

Nectosome: Typically, with small red pigment spots, patches or fine dots scattered over surface; some spots associated with

nectophoral muscular lamellae on dorsal surface ([Figure 4](#)). Maximum nectosome length 230 mm in Villefranche-sur-Mer specimen.

Nectophores: Up to 30 in the largest Pacific specimen observed from the Gulf of California, but commonly much fewer, e.g., 13 in a complete specimen from Villefranche. Surface ridges best displayed in young nectophores ([Supplementary Figure S3](#)), harder to discern in preserved mature nectophores. Young nectophores slightly flattened along upper-lower axis ([Supplementary Figure S3](#)); mature nectophores almost cubical in shape ([Figure 5](#)). Auriculate ridges between upper-lateral and lateral ridges, lying relatively close to ostium on distal surface of young nectophores ([Supplementary Figure S3](#)), nearer top of distal surface in mature nectophores ([Figure 5](#)). Thrust block small in all nectophores examined, at halfway point on proximal surface in young nectophores (not illustrated) and near top of proximal surface in mature nectophores, but with little width overall in proximal-distal plane ([Figure 5](#)). Axial groove in distal mid-line between axial wings in young nectophores ([Supplementary Figure S3](#)). Mature nectophores measuring max. 3.2 mm height \times 3.2 mm width in Villefranche-sur-Mer specimens, max. 3.5mm height \times 3.0 mm width in Peabody Atlantic material; with surface ridges comprising upper-lateral ridge from axial wing tip (on proximal side of nectophore) onto distal nectophore surface, terminating near distal mid-line; auriculate ridge on distal surface, connecting upper-lateral ridge with lateral ridge, and giving off blind-ending side branch; vertical-lateral ridge extending from upper-lateral ridge on upper proximal surface, passing down lateral nectophore surface and inserting on lower-lateral ridge halfway along course of latter; lower-lateral ridge originating at axial wing tip extending along lower-lateral border of nectophore and inserting on lower lateral border of ostium ([Figure 5](#)).

Nectosac with radial canals issuing from the internal pedicular canal. Upper and lower radial canals following straight courses to ostial ring canal on distal surface; lateral radial canals each forming

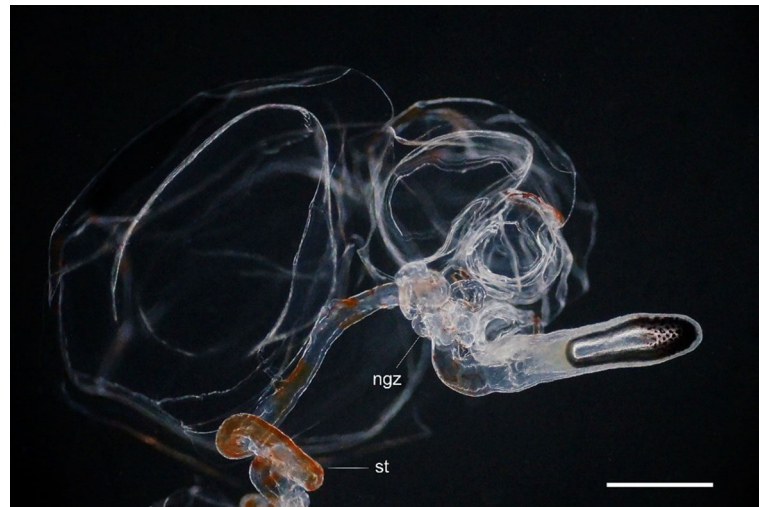


FIGURE 4

Nanomia bijuga pneumatophore and upper nectosome of live specimen from Villefranche-sur-Mer. ngz, nectosomal growth zone; st, stem. Scale bar 1 mm.

first loop on proximal nectosac surface in mature nectophores, passing towards lower surface into second loop, also mostly on proximal surface, then forming third taller loop on latero-distal surface of nectosac, before inserting onto ostial ring canal at level of ostial process on distal nectosac surface (Figure 5). Both ascending and descending mantle canals present, with ascending mantle canal terminating on proximal side of thrust block, and descending mantle canal terminating at junction of proximal and lower

surfaces of nectophore (Figure 5). Small bilobed mouthplate identified in all Peabody Atlantic nectophores, but absent from smaller Villefranche-sur-Mer nectophores. Red spot present on each side of ostium just below level of ostial processes on all Villefranche-sur-Mer nectophores, likely faded to white in Peabody Atlantic nectophores.

Siphosome: Siphosomal stem of Peabody Atlantic specimen c. 10 mm in length, roughly 100 mm in the longest Villefranche-sur-

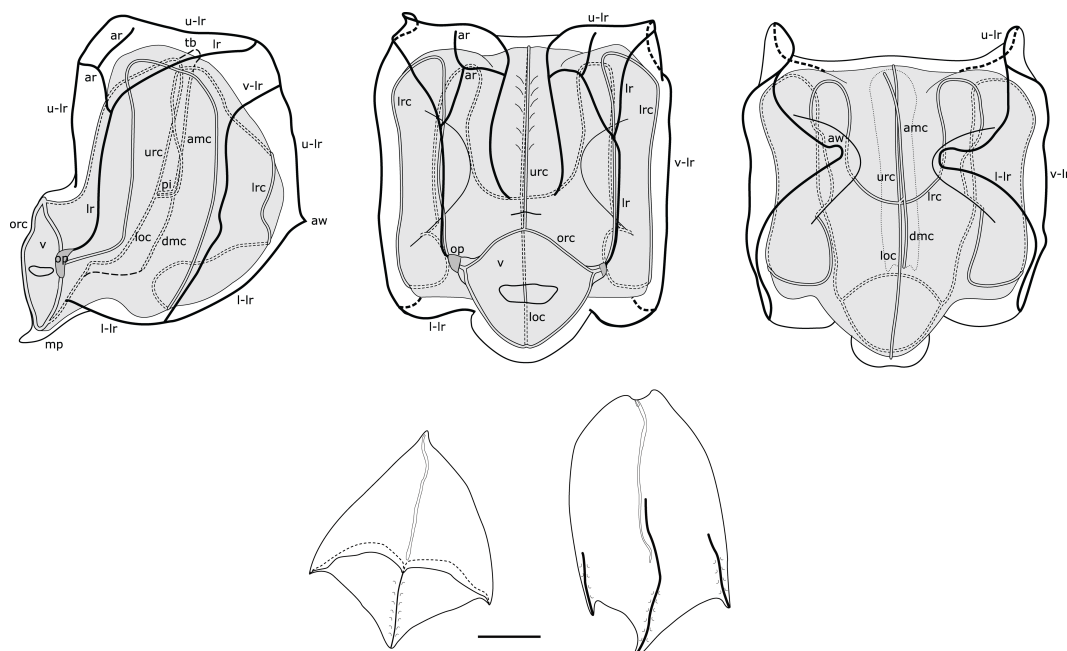


FIGURE 5

Composite illustration of mature *Nanomia bijuga* nectophore and bracts. Lateral, distal and proximal views. amc, ascending mantle canal; ar, auricular ridge; aw, axial wing; dmc, descending mantle canal; loc, lower radial canal; lr, lateral ridge; l-lr, lower later ridge; lrc, lateral radial canal; op, ostial process; orc, ostial ring canal; tb, thrust block; u-lr, upper lateral ridge; urc, upper radial canal; v, velum; v-lr, vertical lateral ridge. 1 mm scale bar for bracts.

Mer specimen measured. Siphosome straight and bearing a number of cormidia with gastrozooids spaced ~5–10 mm apart when pictured in living animals (Figure 6). In younger stem portions cormidia included a single gastrozooid and a palpon, with a number of bracts, whereas the oldest cormidia observed contained four palpons, each with gonodendra of both sexes.

Gastrozooid and tentacle (Figure 6): Gastrozooids mostly elongate in Peabody Atlantic specimen, and all bearing mature tentacles; becoming progressively longer and thinner in more posterior cormidia of Villefranche-sur-Mer colonies (maximum length 1.25 mm) and bearing either larval or definitive tentacles only. In all Villefranche-sur-Mer colonies basigasters pigmented red, though pigmentation faded away in older specimens.

Larval tentilla small (roughly 100 µm), borne on long pedicels and spread far apart. Definitive tentilla larger, borne on longer pedicels and spread further apart. In live specimens from Villefranche-sur-Mer cnidobands pigmented red, mature tentilla comprised three-coiled cnidoband, partial involucrum extending up to the second coil, and long, single terminal filament.

Palpon: All of similar size and typically shorter than gastrozooids in Peabody Atlantic specimen; in Villefranche-sur-Mer specimens, red pigment spots proximally, with thin and elongate palpacle; no lipid droplets discerned in any palpons (Figure 6).

Bracts: Two bract types present (Figure 5), differing in size and shape, probably also in their placement on the stem, but this could not be confirmed.

Type A. Roughly rhomboidal, prismatic and rather small, up to 2.00 mm in length in Villefranche-sur-Mer material. The upper surface divided by a transverse ridge slightly overhanging distal portion, divided into two facets by a median ridge. Bracteal canal narrow, running along the lower surface, from the proximal, bent-upwards process up to the mid-length of bract.

Type B. More elongate and flat, up to 3.00 mm in length in Villefranche-sur-Mer material. The upper surface with three clearly demarcated ridges, of which the median nearly twice the length of the lateral ones. All ridges were elevated, and contained large cells, potentially nematocysts, and ended in distinct cusps giving the bract a tridentate appearance. In some bracts the distal cusps were elongated. In younger bracts weak ridges connected lateral ridges with the median ridge, but they could not be discerned in older bracts. The bracteal canal proximally bent upwards onto the bract's upper surface, running along the lower surface of bract up to 2/3 of its length.

Gonodendra: Monoecious, with both female and male gonodendra found within each mature cormidium (Figure 6). Gonophores of both sexes with clear orange pigmentation in living specimens; pigmentation lost in fixed animals.

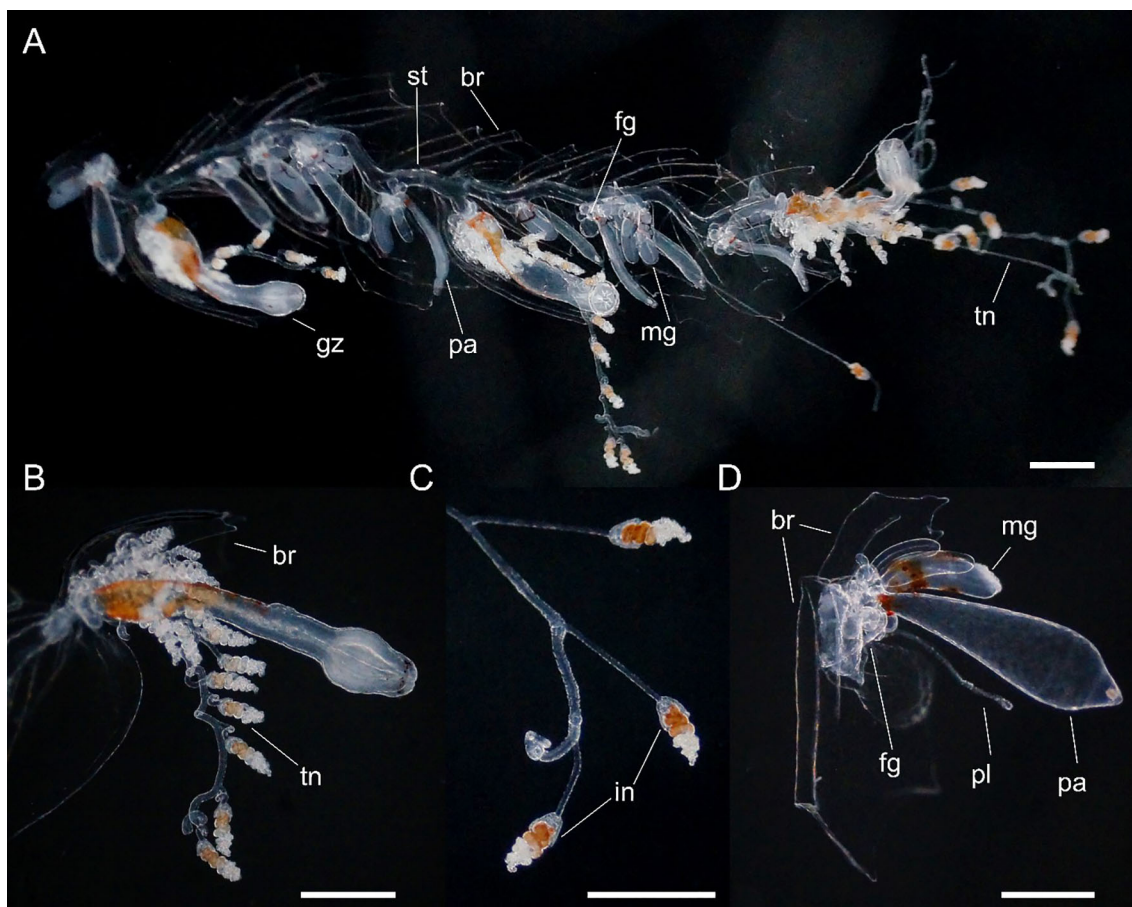


FIGURE 6

Nanomia bijuga (A) portion of siphosome, (B) gastrozooid, (C) tentilla and (D) palpon. Live specimen from Villefranche-sur-Mer. br, bract; fg, female gonophore; gz, gastrozooid; in, involucrum; mg, male gonophore; pa, palpon; pl, palpacle; st, stem; tn, tentacle. Scale bars 1 mm.

Distribution

The type locality of *Nanomia bijuga* (original name *Physsophora bijuga* Delle Chiaje, 1844) is the Gulf of Naples. In addition to all our specimens from the Mediterranean, specimens from the Gulf of California and Hawaii were identified as *N. bijuga*, confirming the presence of the species in North Atlantic and low-latitude Pacific waters (Figure 2). In addition, sequences originating from off Virginia (GenBank accession AY937373) and Bermuda (GenBank accession GQ120022) as well as Korean waters (Park and Lee, 2022) were molecularly confirmed as *N. bijuga*. According to Totton (1954) *N. bijuga* is distributed in the Tropical Atlantic, Mediterranean, West Indian, Indian Ocean and warm-water Pacific.

Remarks

The auriculate ridge, which is here identified as being a diagnostic character of *N. bijuga* proper, was clearly present in Totton's specimens from Villefranche-sur-Mer (Figures 32 & 34 in Totton, 1965), and in our material from Northern Adriatic, the re-examined Peabody Atlantic specimen from off Virginia, and our specimens from the Gulf of California and Hawaii. Auriculate ridges have also been described from the Benguela current (Pages and Gili, 1992) and the South Atlantic (Figure 3.14 in Pugh, 1999), as well as in material collected from the Indian Ocean, off Zanzibar (Mapstone, 2009). In the Pacific Ocean, Kawamura (1911) illustrates auriculate ridges in the west Pacific specimens he studied at Misaki marine station in Japan (reproduced in Pl. X in Totton, 1965), while Agassiz and Mayer (1902) describe specimens with auriculate ridges from Funafuti Atoll, Tuvalu, as *Anthemodes moseri*. These observations suggest that the distributional range of *N. bijuga* may well be considerably wider than documented by the current study. However, due to the existence of the two as of yet morphologically undescribed lineages, it is unclear whether the auriculate ridges will remain a diagnostic character for *N. bijuga* alone.

Our data also indicate undescribed intraspecific molecular and morphological variation between populations of this widespread species, warranting closer scrutiny. Agassiz and Mayer (1902) also noted that the Pacific specimens in many respects differ from the Atlantic ones. For example, the specimens from the Gulf of California and Hawaii have ~30 nectophores (Supplementary Figure S4), making them veritable giants compared to the Mediterranean specimens commonly observed.

The history of *N. bijuga* is convoluted. The original description is rather vague, based on just a few figures (Delle Chiaje, 1844), and there are at least 14 wholly or partly synonymized names (Schuchert, 2024, also see Mapstone, 2009). Here, we provide, for comparative purposes, a description of the material examined for this study only (Supplementary Table S1), and keep to the currently established nomenclature. It should be noted that we have not examined type material for *N. bijuga* (if it exists) or any of the synonymized species, nor have we examined material from the type locality in the Bay of Naples.

3.2.2 *Nanomia cara* A. Agassiz, 1865

Material examined is specified in Supplementary Table S1.

Diagnosis. Longitudinal septa in pneumatophore indistinct; nectosome with red pigment spots in life (yellow when preserved). Mature nectophores flattened along upper-lower axis, orthogonal to

stem axis, resulting in elongate proximal-distal axis and short upper-lower axis; axial wings extending along this axis to beyond stem attachment point, without axial groove; no auriculate ridge connecting upper-lateral ridge with lateral ridge; thrust block extensive in larger nectophores. Palpon with proximal lipid droplet.

Barcode Index Number (BIN) in BOLD: ACQ6137.

Description

Pneumatophore: Up to 2.0 mm long (in preserved specimens), with red pigmented apex when alive (Figure 7), remainder transparent with gas gland occupying posterior half to one third and opaque white in present material. Occasional very thin irregular longitudinal lines, one or more, observed on surface. Apical pore present.

Nectosome. Nectosomal stem bearing yellow-red pigment spots scattered over ventral surface at anterior end and continuing along nectosome as two faint pigmented lines to two thirds or more of total length in live images from large Gulf of Maine colony (Figure 7); bearing red pigment spots at anterior end in nectosome of smaller live colony from Rocky Bay; yellow spots also discernible in some preserved nectosomes from Norwegian material. Nectophores arising from nectophoral muscular lamellae on dorsal surface only; nectophores typically detach at preservation due to contraction of specimen.

Nectophores: Nectophores colorless, shape changing with size (Figure 8). Smallest nectophores approximately cubical, without conspicuous proximal axial wings, reminiscent of *N. bijuga* (Figure 8, also see Figure 2 (as *N. bijuga*) in Haberlin et al., 2016). Largest nectophores reaching 8.7 x 11.3 mm max length by width, conspicuously flattened along the upper-lower axis and with conspicuous axial wings (Figures 8, 9). 15 mature nectophores present in live Gulf of Maine specimen (Figure 7).

Ridge pattern similar in all well-preserved nectophores (Figure 9): upper-lateral ridges originating at proximal tip of axial wing, extending distally along upper outer edges of nectophore to highest point (in lateral view) or a short way distal of it, passing onto upper nectophore surface, continuing diagonally towards distal mid-line for a short distance and terminating near latter; lateral ridges originating from upper-lateral ridges, curving downwards onto lateral nectophore surface and inserting onto ostium at ostial process; lateral ridges relatively longer in smaller, young nectophores than in larger, older ones. Vertical-lateral ridges originating from upper-lateral ridges, extending distally diagonally down lateral sides of nectophore and inserting onto lower-lateral ridge about halfway along its length; lower-lateral ridges extending from near end of axial wing along lower outer edge of nectophore and in mature nectophores inserting onto lower-lateral borders of ostium.

Nectosac well-rounded in young nectophores, y-shaped and extending into axial wings in older larger nectophores (Figure 8). Radial canals issuing from the internal pedicular canal (sometimes staggered). Upper and lower radial canals straight, lateral radial canals forming two upward loops en route to ostium including a proximal loop upwards from the junction, and a second upward loop on lateral nectosac surface, inserting onto ostial ring canal at position of ostial process. Ascending and descending mantle canal present; the ascending mantle canal extends up to the thrust block

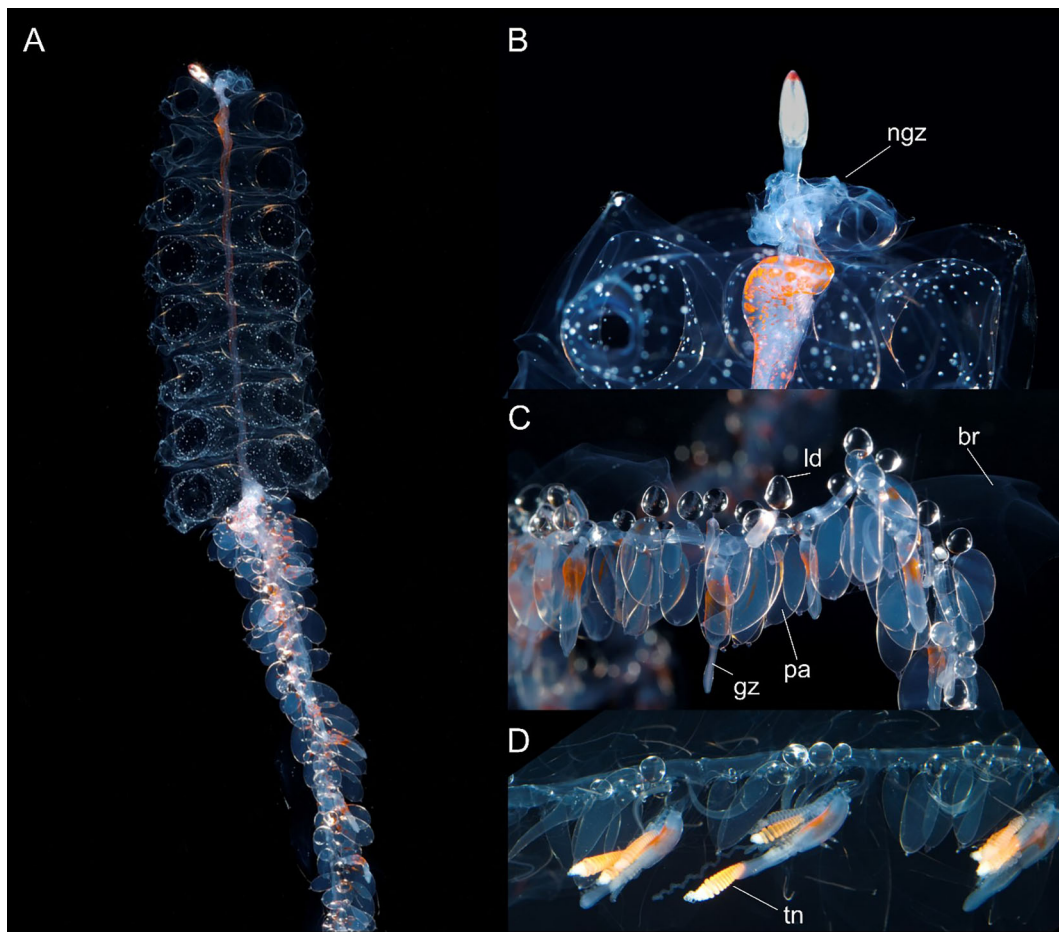


FIGURE 7

Nanomia cara (A) colony, (B) pneumatophore and upper nectosome, (C, D) parts of siphosome. br, bract; gz, gastrozooid; ld, lipid droplet; ngz, nectosomal growth zone; pa, palpon; tn, tentacle. Live specimen from Gulf of Maine. White spots on nectophores not typical, may be air bubbles resulting from sample processing. Photos by David Shale.

and the descending mantle canal passes down towards nectophore's lower surface.

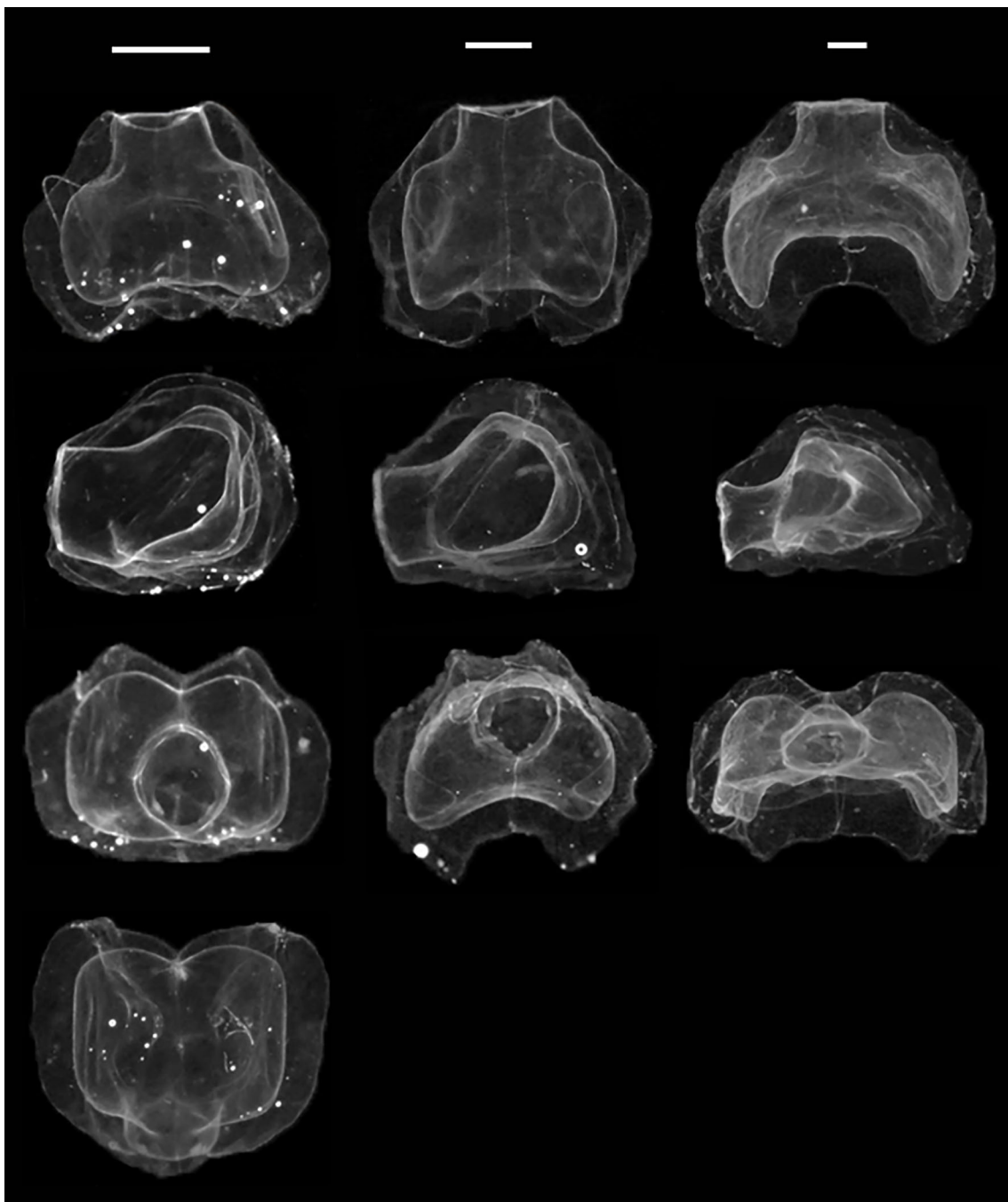
Thrust block identifiable in small nectophores from outside Cork Harbour, Ireland, as small dome-shaped protrusion between axial wings (in upper view). As nectophore grows larger and axial wings move further apart (in Arctic and Norwegian specimens), thrust block broadens and protrudes further from proximal surface of nectosac (in upper view). In some very large Arctic nectophores, the thrust block may dome out beyond proximal ends of axial wings in upper view, while in others it remains level with axial wings; a thrust block can also be identified as a large structure in lateral views of mature nectophores, extending from the upper proximal surface. In some nectophores from the Arctic, thrust block shorter than axial wings in upper view, but mesogloea still thickened in this region. This is illustrated by the relatively extensive length of the internal pedicular canal.

Siphosome: Cormidia easily discerned on siphosomal stem of the large colony from Gulf of Maine, delimited anteriorly by an elongate gastrozooid with a broad band of orange-red pigment near its proximal end and contracted tentacle with prominent tentilla (Figure 7). Most cormidia in these images comprising 4–5 palpons

(identifiable by their single proximal lipid droplet), and numerous bracts. No gonodendra identified in specimen in Figure 7, suggesting it was not yet sexually mature.

Gastrozooid and tentacle: Small spot of orange pigment near proximal end of gastrozooids of Rocky Bay specimen, with more similar spots present in Norwegian gastrozooids. In larger gastrozooids from the Gulf of Maine 2015 colony, orange-red pigment more extensive in the proximal half of the zooid (Figure 7). Many larval tentilla developing at proximal end of basigaster in young Bantry Bay gastrozooids, but no definitive tentilla. Larval tentilla also associated with some tentacles of Rocky Bay specimen, but most tentilla on this latter specimen definitive with 2–3 coiled orange cnidoband enclosed by partial involucrum and single relaxed long terminal filament when alive. Tentilla with 5–8 coils were observed on a live specimen from Bergen, while 10–11 coils were present throughout siphosome of Gulf of Maine specimen (Figure 7); most pigmented orange red, but a few transparent.

Palpons: From 1.0 to 4.0 mm max length in present material; most containing proximal lipid droplet, becoming prominent in large palpons (Figure 7); palpons all opaque in preserved material with thin palpacle emerging from proximal end. In young Bantry

**FIGURE 8**

Ontogenetic change in *Nanomia cara* nectophore shape. Upper/lower, lateral, distal and proximal views (top to bottom). Specimens (left to right): HYPNO_050, HYPNO_037, HYPNO_122 (ref. [Supplementary Table S1](#)). Scale bars for each column ~1 mm.

Bay palpons, lipid droplets identified forming in column of palpon, presumably migrating proximally, and eventually coalesced into single proximal lipid droplet.

Bracts: Two types of bracts present ([Figure 9](#)): Type A kite-shaped and Type B, found in enantiomorphic pairs.

Type A. Kite-shaped, longer (2.0 mm) than wide (1.6 mm). Distinctly prismatic, often as high as wide. With an obvious cell patch on the upper surface, prone to abrasion hence lost in some bracts. Such patches have been shown to be the sites of

bioluminescence in other physonects. Distally the upper surface divided into two facets, separated by a prominent median ridge. Two other ridges demarcating lateral margins of distal facets. Median ridge and lower third of lateral ridges lined with large cells. Bracteal canal running along lower surface without penetrating into mesoglea for nearly 80% of bract's length, but not reaching the proximal process.

Type B. More elongate than Type A, reaching 1.6 mm in length and 0.9 mm in width. Terminating distally in three cusps. Three

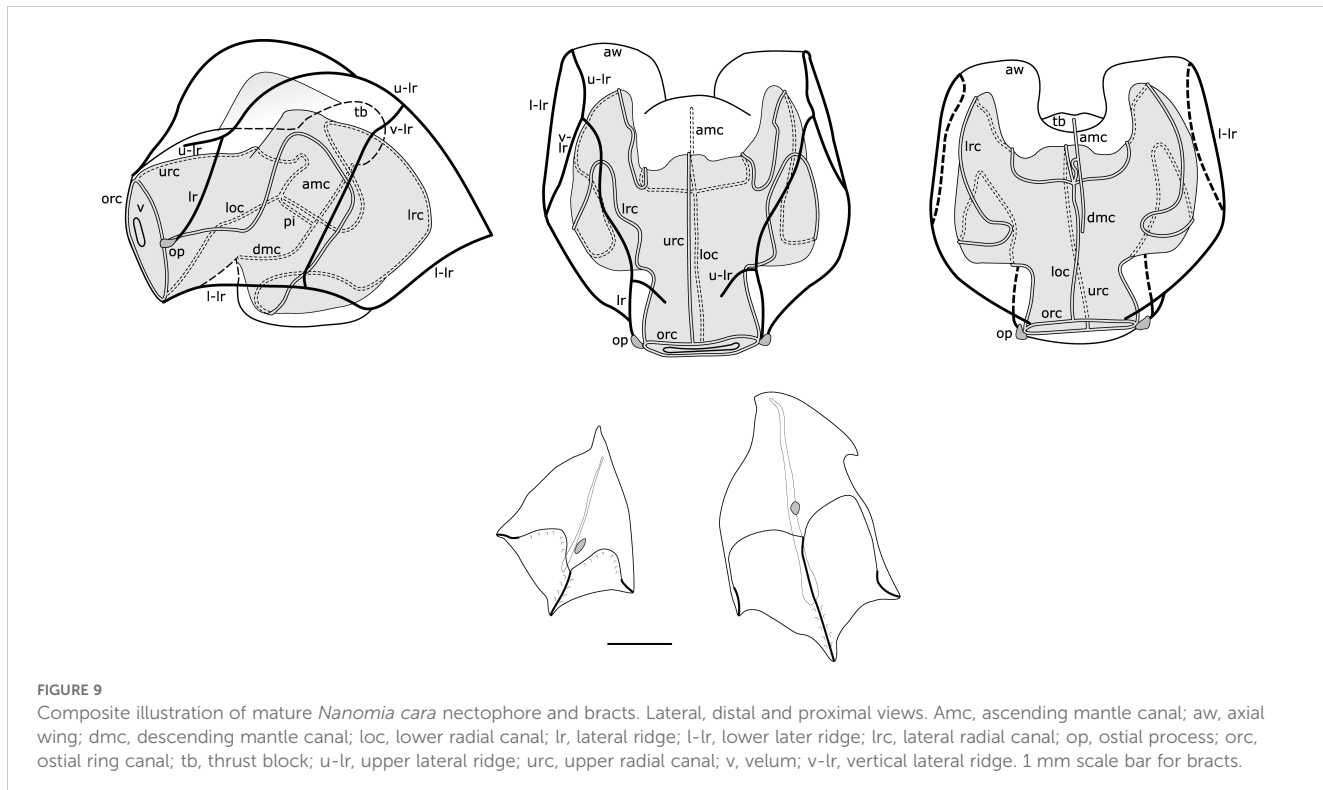


FIGURE 9

Composite illustration of mature *Nanomia cara* nectophore and bracts. Lateral, distal and proximal views. Amc, ascending mantle canal; aw, axial wing; dmc, descending mantle canal; loc, lower radial canal; lr, lateral ridge; l-lr, lower later ridge; lrc, lateral radial canal; op, ostial process; orc, ostial ring canal; tb, thrust block; u-lr, upper lateral ridge; urc, upper radial canal; v, velum; v-lr, vertical lateral ridge. 1 mm scale bar for bracts.

nearly parallel ridges run from those cusps up to the half of the bract's length. Entire median ridge and roughly one third of lateral ridges lined with prominent cells. Lateral ridges appear to connect with median ridge in younger bracts, connection was indistinguishable in older zooids. Proximally additional lateral cusp on a single side of the bract. Single cell patch on the bract's upper surface. Bracteal canal not originating on the proximal process, running along the lower surface of bract for nearly 80% of bract's length. Bracts found in enantiomorphic pairs, with the proximal cusps displaced either on left or right side; sometimes one of the distal lateral cusps longer than the other one.

Distribution

Material from current study confirms the distribution of *N. cara* in the NE Atlantic around the British Isles, in the North Sea, along the Norwegian coast and in the Atlantic water masses of the Arctic. GenBank sequences from the Gulf of Maine, NW Atlantic, were also verified as belonging to *N. cara*, corresponding with the type localities in Massachusetts Bay, Nahant, and Newport, R. I (Agassiz, 1865). This agrees with the distribution proposed by Totton (1954).

Remarks

The examined material shows an ontogenetic change in the shape of the nectophores (Figure 8), which is likely partly responsible for the confusion surrounding the identity of NE Atlantic *Nanomia*. The general shape and habitus of smaller nectophores is more reminiscent of that of *N. bijuga*, with the nectophores assuming the horizontally flattened form associated with *N. cara* (cf. Totton, 1954 and reproductions thereof) as they mature and grow. As the nectophores grow, the axial wings become

more prominent, with the nectosac extending into them. The upper lateral ridges get displaced laterally, and the nectophores become somewhat flaccid, with the ridges less conspicuous. The colonies originally described by Agassiz (1865) were small and likely immature, with a maximum of eight nectophores. The original description of the small nectophores tends towards the intermediate type typical of young *N. cara* nectophores, rather than mature *N. cara* nectophores as illustrated by Totton (1954). The syntype (not examined for this study) from Nahant is catalogued at Harvard University's Museum of Comparative Zoology' Invertebrate Collections under the catalogue number CNID-1745, with condition set as "poor".

As with *N. bijuga*, there appears to be potential morphological variation between populations, with large specimens up to 1 m in length having been reported from the Gulf of Maine (Rogers et al., 1978). In this study, the specimen from the Gulf of Maine was observed to have more cnidoband coils than the specimens examined from other regions, suggestive of a larger size, even though the specimen was apparently still sexually immature.

3.2.3 *Nanomia septata* sp. n.

Illustrations of *N. septata* sp. n.

As *Nanomia bijuga*: Mapstone, 2009 (Figure 20), Mapstone and Arai, 1992 (Figures 3, 4), Church et al., 2015 (Figures 1–6), Norekian and Meech, 2020 (Figure 1, 2), Siebert et al., 2011 (Figure 1), Siebert et al., 2015; Sutherland et al., 2019.

As *Nanomia cara*: Mackie, 1963 (Figure 24-1), Mackie, 1964 (Figures 1–7), Mackie, 1986 (Figure 10), Freeman, 1987 (Figures 3–6).

Etymology: specific name *septata* (f.) is latin for having a septum or being septate, with reference to the conspicuous longitudinal septa in the pneumatophore of fixed specimens of the species.

Authorship: Recommended citation “Mapstone, Mańko, Martell, Haddock & Hosia in Hosia et al., 2024”.

Material examined is specified in [Supplementary Table S1](#).

Yale Peabody Museum specimen with catalogue number YPM IZ 111054 is designated as holotype and YPM IZ 35043 as paratype (see [Supplementary Table S1](#)).

Diagnosis. Pneumatophore with < 14 conspicuous longitudinal septa; nectosome with orange pigment (in live material). Nectophores flattened along proximal-distal axis when mature, parallel to stem axis, with prominent pigmentation of ostial region in living colonies; axial wings bent over on proximal side, partly enclosing stem; no auriculate ridge connecting upper-lateral ridge with lateral ridge; thrust block small and insignificant in all nectophores. Palpons with elongate palpacle, lipid droplet inconspicuous if present.

Barcode Index Number (BIN) in BOLD: ACL8638.

Description

Pneumatophore: Pneumatophore up to 5 mm long, apex with red pigment, outer wall typically with 12-13 conspicuous longitudinal septa from apex to base ([Figure 10](#)); gas gland pinkish in Vancouver Island pneumatophores.

Nectosome: With prominent orange pigmentation in living animal ([Figure 10](#)), and nectophores budding off dorsally; 11 fully developed nectophores were found with the holotype ([Figure 10](#), a single nectophore detached prior to taking picture).

Nectophores: Young and mature nectophores of holotype in good condition. In distal view young nectophores 2.25 x 2.25 mm, mature nectophores 5.0 mm x 4.5 mm (max height x width); young nectophores with axial wings tall in distal view and separated by deep cleft ([Figure 10](#)); mature nectophores with axial wings shorter in distal view, separated by a shallower cleft ([Figure 11](#)); axial wings folded inwards on proximal side of nectophore, touching in Peabody Pacific specimen or not touching in other material (not illustrated). Outer surface smooth in all Peabody Pacific nectophores, with ridges easily discerned, but courses best illustrated in composite drawings from several mature nectophores ([Figure 11](#)). Incomplete upper-lateral ridges originating at axial wing tip, passing upwards and outwards to

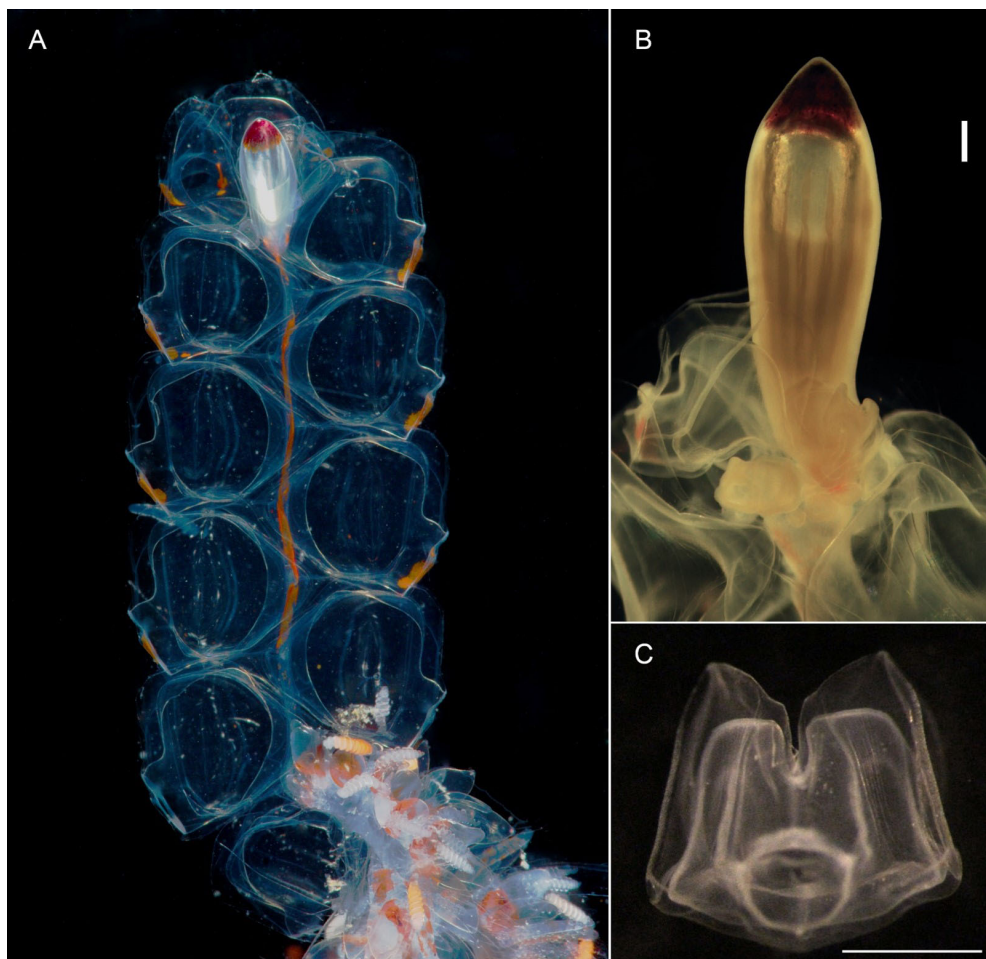
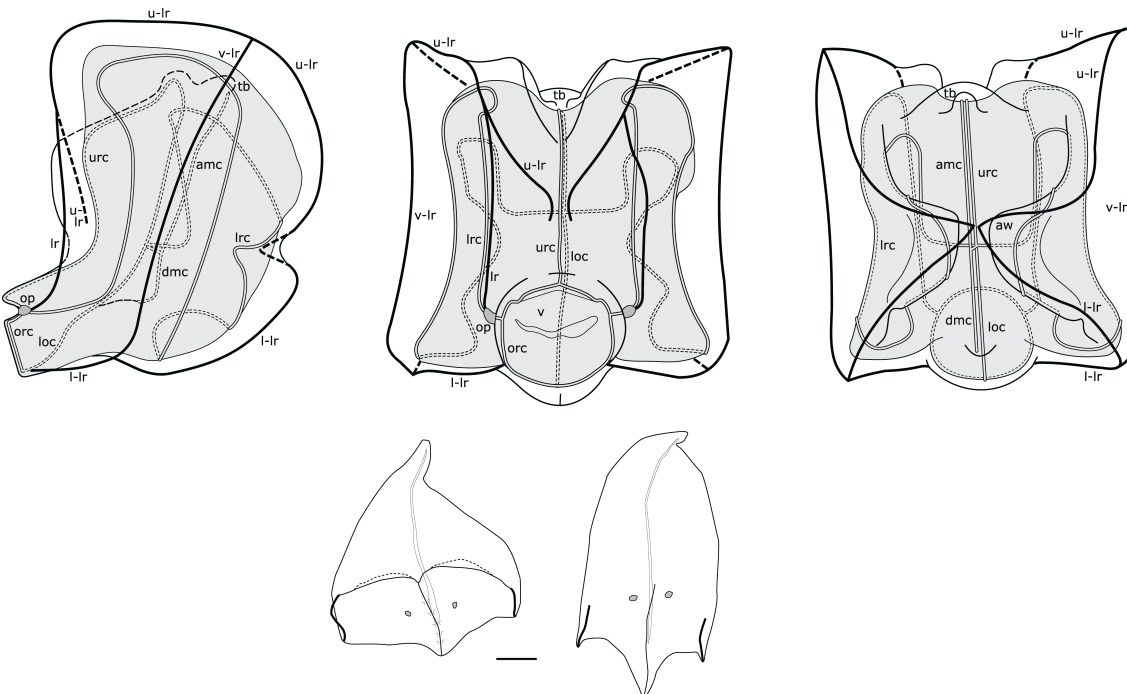


FIGURE 10

Nanomia septata sp. n. (A) nectosome (live holotype), (B) pneumatophore (holotype after fixation), scale bar 500 µm and (C) young nectophore (paratype), distal view, scale bar 1 mm.

**FIGURE 11**

Composite illustration of mature *Nanomia septata* sp. n. nectophore and bracts. Lateral, distal and proximal views. amc, ascending mantle canal; aw, axial wing; dmc, descending mantle canal; loc, lower radial canal; lr, lateral ridge; l-lr, lower later ridge; lrc, lateral radial canal; op, ostial process; orc, ostial ring canal; tb, thrust block; u-lr, upper lateral ridge; urc, upper radial canal; v, velum; v-lr, vertical lateral ridge. 1 mm scale bar for bracts.

upper lateral nectophore surface and then downwards and inwards on distal surface terminating near distal mid-line at about half nectophore height (Figure 11); vertical-lateral ridges passing from high point of upper-lateral ridges diagonally down lateral nectophore surfaces to insert on lower-lateral ridge; lateral ridges extending from upper-lateral ridges on distal surface and passing down to insert on lateral borders of ostium at level of ostial process; lower-lateral ridges extending from tips of axial wings, along lower lateral surfaces of nectophore to insert at ostium below lateral ridges.

Nectosac extensive in all nectophores (Figures 10, 11); radial canals originating from junction with internal pedicular canal on proximal surface; upper radial canal straight, passing through V-shaped cleft onto distal surface, downwards in mid-line and inserting onto ostial ring canal; lower radial canal following similar straight course along lower surface of nectosac to ostial ring canal (Figure 11); lateral radial canals following sinuous looped courses from junction with internal pedicular canal, first forming upward loop on proximal nectosac surface, then lower loop on proximal to lower-lateral surface, and finally taller loop on latero-distal nectosac surface before descending and inserting onto ostial ring canal in lateral position (Figure 11).

Short internal pedicular canal giving rise to both ascending and descending mantle canals. Ascending mantle canal extending upwards from junction to middle of thrust block in proximal view, and descending mantle canal extending downwards to point where lower mid-line of nectosac turns through 90° (Figure 11).

Thrust block terminating just below upper surface of nectosac in proximal view of mature nectophores (Figure 11), halfway up proximal surface in young nectophores (not illustrated).

Siphosome: Siphosomal stem with the cormidial arrangement typical of the genus, with gastrozooids followed by several palpons, each flanked by both a female and a male gonodendron on alternate sides (Figure 12).

Gastrozoooid and tentacle: Gastrozooids with distinctly orange proximal one third, elongate, reaching up to roughly 7.0 mm in length (Figure 12). With prominent hepatic stripes. Tentilla with long pedicels (Figure 12), with 8 cnidoband coils when mature and single terminal filament. Involucrum incomplete, covering 2-5 coils of cnidoband (Figure 12). In live specimens cnidoband distinctly orange. No larval tentilla identified in present material.

Palpon: Elongate, up to 7.0 mm long, nearly 1.2 mm wide, narrowing down distally (Figure 12). All palpons with proximally attached palpacle. Some palpons with an internal proximal droplet, possibly containing lipids.

Bracts: Two types of bracts present (Figure 11). As in other *Nanomia* species, one more prismatic, roughly rectangular, and other tricuspidate and elongate. Both types with two cell patches.

Type A. Prismatic, 5.5 mm long and 5.0 mm wide. The upper surface divided in two by a transverse ridge running from distal cusps up to one third of bract length. The transverse ridge forming minute overhangs above the distal surface. The distal surface divided into two facets by a median ridge connecting with the transverse ridge. Each of the two distal facets with a distinct cell

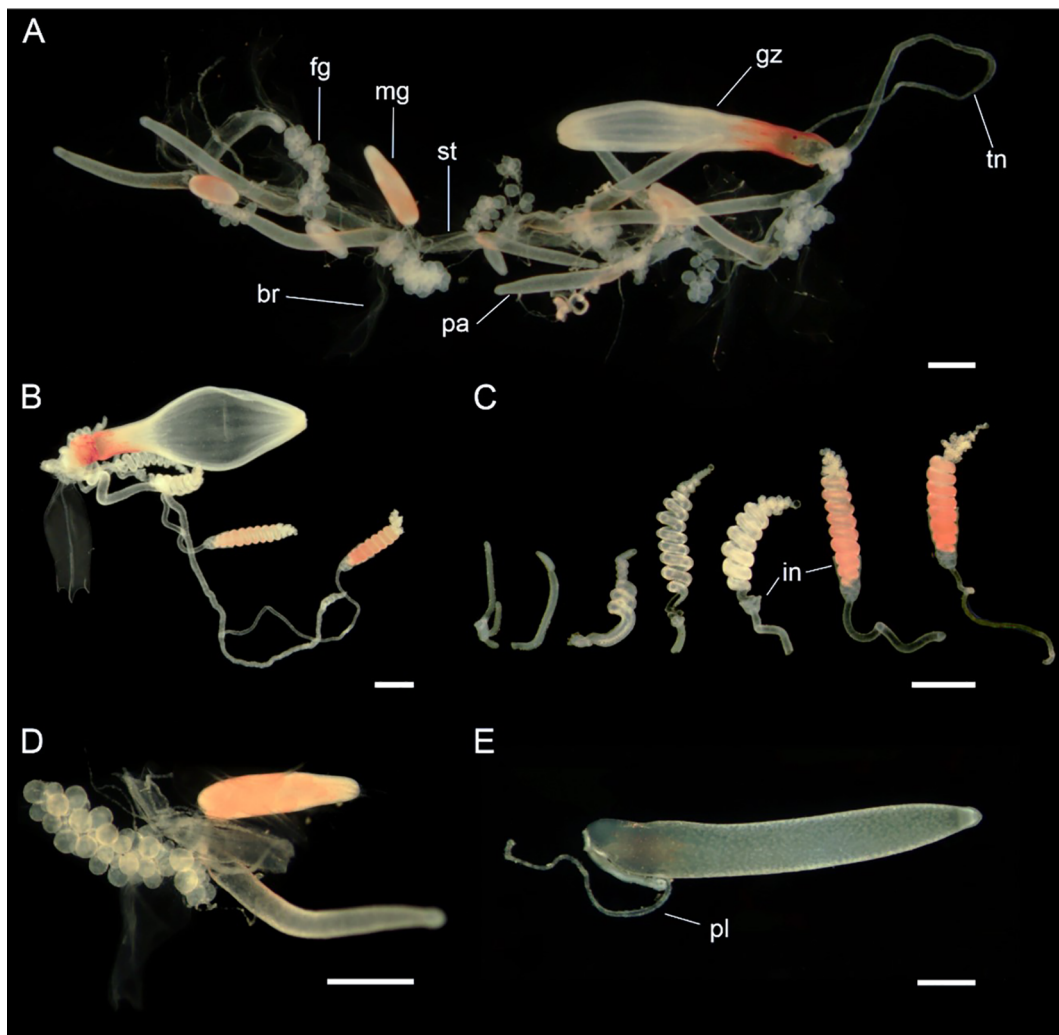


FIGURE 12

Siphosomal zooids of *Nanomia septata* sp. n. holotype. (A) Cormidium showing gastrozooid and groups of palpon with female and male gonodendra on alternate sides, (B) gastrozooid, (C) tentilla from a single tentacle, from youngest to oldest (left to right) in various stages of development, (D) female and male gonodendra on either side of a palpon, and (E) palpon with palpacle. br, bract; fg, female gonophore; gz, gastrozooid; in, involucrum; mg, male gonophore; pa, palpon; pl, palpacle; st, stem; tn, tentacle. Scale bars: 1 mm.

patch. Lateral portion of a transverse ridge lined with larger cells. Bracteal canal originating on the proximal process and running nearly to the distal tip of the bract.

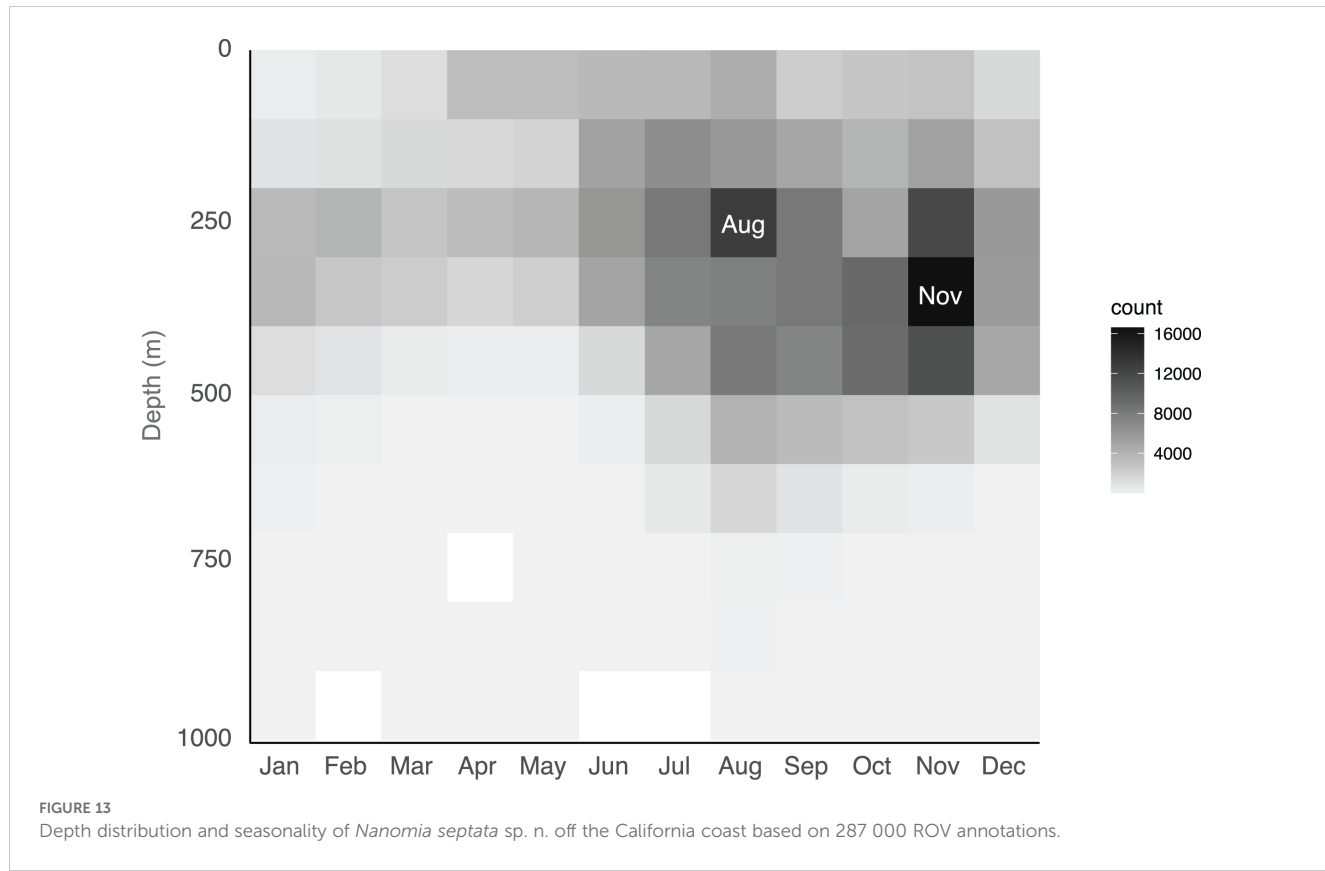
Type B. Elongate, 6.3 mm long and 2.0 mm wide. Terminating with three cusps, each with a ridge running towards proximal portion of bract. Lateral ridges much shorter than the median ridge, and lined with distinct cells. Median ridge longer, running up to one third of bracts upper surface, not lined with any cells, and with distinct cell patches, one per side of the ridge. Bracteal canal started near the proximal process and run along the lower surface for the majority of bracts length.

Gonodendra: Monoecious, with both male and female gonodendra attached at bases of individual palpons (Figure 12). Male gonophores elongate, white when immature, becoming orange upon maturation. Female gonophores small, oval, each with a single egg cell.

Distribution

Molecular identification confirmed the presence of *Nanomia septata* in the North Pacific, from California up to Vancouver in the east, as well as from Japanese waters in the west. *Nanomia septata* is extremely abundant in the eastern North Pacific, spanning from the surface to 550 m, based on 287 000 ROV annotations gathered over a 30-year period (Figure 13). The mean number of specimens observed on each ROV dive was 234, with a maximum of 3997. The bulk of the sightings occur at daytime-depths between 200 and 450 m. Although depth data were primarily obtained during the day the distribution is not constant since *Nanomia* undergo diel vertical migration, to maximize overlap with their predominant prey of krill (Choy et al., 2017). *N. septata* are most abundant between August and November, and there is a potential seasonal shift during development, since the depth of occurrence increases from August to November (Figure 13).

Remarks



Nanomia septata sp. n. has likely been mistakenly identified as both *N. cara* and *N. bijuga* in several publications from the North Pacific. This is definitely the case for the publications from which the sequences used in this study stem (Supplementary Table S1), as well as other studies that have used these specific sequences as *N. bijuga*. In particular, *N. bijuga* from the US west coast – here considered *N. septata* – has been used as a model organism in several evo-devo and other studies (e.g. Spencer, 1971; Siebert et al., 2011; Church et al., 2015; Siebert et al., 2015; Sutherland et al., 2019; Norekian and Meech, 2020). Where genetic data or suitable tissue is available, the identity of the *Nanomia* species in such papers can be checked by comparing with the COI and 16S sequences from the present study. It should be noted that *N. septata* sp. n. appears to occur in close proximity to several other species of *Nanomia* – with *N. bijuga* towards its southern range along the North American coast, with *N. bijuga* and the undescribed sp.1 in Japan, and with undescribed sp.2 also observed in the north-west Pacific—necessitating care when identifying specimens morphologically.

One of the characters separating the *Nanomia* species is the presence and appearance of a proximal lipid droplet on the palpons (Table 1). *Nanomia cara* typically display prominent external droplets (Figure 7), while the *N. bijuga* proper do not have such lipid droplets (Figure 6). The hitherto unresolved taxonomy has caused confusion also in this matter. Church et al. (2015) questioned the validity of this character in separating *N. cara* and “*N. bijuga*” (in fact *N. septata*) and reported on a large, proximal lipid droplet creating a pronounced protrusion on the palpons of *N. septata* (as “*N. bijuga*”) in their histological study (see Figure 4 in

Church et al., 2015). However, according to our observations, the lipid droplets in *N. septata* remain largely internal to the palpons (Figure 12), resulting in a slight protrusion in the proximal end of the palpon but never forming a conspicuous external body as in *N. cara* (Figure 7).

The complex history and widespread distribution of *Nanomia* siphonophores renders any systematic treatment difficult. The generic name *Nanomia* was introduced by Agassiz, 1865 for *N. cara* collected off Massachusetts. The name, however, is actually preceded by both Cupulita Quoy and Gaimard, 1824 and Agalmopsis Sars, 1846, with *Cupulita* having priority. To add to the confusion, the description of *Agalmopsis elegans* Sars, 1846 was based on specimens of two species, currently known as *N. cara* and *Agalma elegans* (Sars, 1846). This would imply that not only the name *Nanomia* should be replaced with *Cupulita*, but also that the specific name *cara* should be suppressed by *elegans* (currently in use for another species in the same family: *A. elegans*). However, both *N. cara* and *N. bijuga* meet requirements of the International Code of Zoological Nomenclature article 23.9. on reversal of precedence, thus allowing us to retain them.

The Pacific *Nanomia* species, which we describe here under the name *N. septata* sp. n., has been reported earlier as *N. cara* (e.g., Mackie, 1964), *N. bijuga* (e.g., Church et al., 2015) or simply as *Nanomia* (e.g., Mackie, 2002). To the best of our knowledge, the only *Nanomia*-like siphonophores with a type locality in the Pacific Ocean are *Cupulita boodwiche* Quoy and Gaimard, 1824 and *Anthemodes moseri* Agassiz and Mayer, 1902 [currently synonymized with *N. bijuga* (Delle Chiaje, 1844)]. The former was collected from Port

Jackson, Australia, its description is vague, and the species is considered a *taxon inquirendum* in the World Hydrozoa Database (Schuchert, 2024). The latter was collected off Tuvalu (tropical Pacific), and differs in morphology from *N. septata* sp. n. Given the lack of documented morphological similarity with the above species and the considerable geographic distance to their type localities, the magnitude of unresolved diversity of Pacific *Nanomia* (e.g., Figure 3), as well as the convoluted systematics of *Nanomia*, we consider it justified and prudent erect a new species for *N. septata*.

4 Discussion

Several factors have served to make assigning *Nanomia* specimens to the previously accepted species *N. bijuga* and *N. cara* challenging. The existence of several, hitherto morphologically undescribed lineages has certainly impeded correct identification of *Nanomia* from the Pacific. Furthermore, the focus on the identification between *N. bijuga* and *N. cara* has largely been on the axis of flattening of the ectophores, but this character is somewhat subjective and does not account for the ontogenetic changes in the morphology of *N. cara* ectophores, thus leading to erroneous conclusions about younger ectophores in particular. A better character to separate the species is the arrangement of the ridges on the upper surface of the ectophores, as described in the current paper (Table 1; Figures 5, 9, 11).

We suggest that the so-called auriculate ridge joining the lateral and upper lateral ridges of the ectophores, which Totton (1965) describes from some, but not all, *N. bijuga* individuals, is indeed a diagnostic character for *N. bijuga* proper. Such auriculate ridges are absent from all Pacific specimens now considered *N. septata* sp. n., as well as all Atlantic *N. cara*. The species also differ in terms of the relative placement of the junction between the lateral ridge and the upper lateral ridge.

Another point of confusion has been the presence of oil droplets at the base of the palpons. Our data suggests that conspicuous, external oil droplets are only present in *N. cara*, while any such droplets in *N. septata* remain internal to the palpon, only resulting in a slight protrusion (also see Church et al., 2015). No oil droplets were observed in *N. bijuga*. Finally, *N. septata* sp. n. clearly differs from both other species in terms of the conspicuousness of the septa in its pneumatophore.

Our results clarify that the *Nanomia* commonly observed in NE Atlantic waters is predominantly *N. cara*, as previously suggested by several authors (Totton, 1954; Kirkpatrick and Pugh, 1984; Hosia and Båmstedt, 2008; Knutsen et al., 2018). That being said, advection of siphonophores and other pelagic hydrozoans with a more southern distribution into the North Sea and along the Norwegian coast is not an uncommon occurrence (Båmstedt et al., 1998; Edwards et al., 1999; Fosså et al., 2003), so we cannot completely dismiss the validity of all *N. bijuga* observations from these waters. Nevertheless, all our samples from Irish waters are unequivocally *N. cara*, rather than *N. bijuga* as proposed by Baxter et al. (2012) and (Haberlin et al., 2016, 2019). Incidentally, the most commonly reproduced illustration of *N. cara* ectophores, originally from Totton (1954), is based on a specimen collected at Valentia Island, Ireland.

The morphology of *N. cara* ectophores is shown to change during ontogeny and growth, with the smaller and younger ectophores generally having a more intermediate shape reminiscent of *N. bijuga*. As the size of the colonies at this point is also closer to that typical of *N. bijuga* from Atlantic and Mediterranean waters, it can be difficult to morphologically tell apart the two species in this size range based on general ectophore habitus or the plane of flattening. The small size (0.5–2 mm in diameter) of the ectophores examined by Baxter et al. (2012) could have contributed to a potential misidentification based on morphology. Baxter et al. (2012) also confirmed their identification by comparing 18S sequences with those from a presumed *N. bijuga* from the Pacific, but as the sequences were not published, we have been unable to verify their identity. A re-evaluation of these results would be interesting, as we now know that there are multiple species of *Nanomia* present in Pacific waters. 18S sequences are also highly conserved within cnidarians (Berntson et al., 1999; Cartwright et al., 2008). The results from Baxter et al. (2012) in combination with the shape of the ectophores led Haberlin et al. (2016) to misidentify their Irish specimens as *N. bijuga*, though they also stated that the material showed a marked similarity to the early descriptions of *N. cara* (Agassiz, 1865; Fewkes, 1888). These ectophores were also only up to ~1.4 mm in width, and the photos of the colony from Bantry Bay show small *N. cara* ectophores of an intermediate morphology (as *N. bijuga*, Figure 2 in Haberlin et al., 2016).

Morphological variation in colony size and other characteristics has previously been reported for both *N. cara* and *N. bijuga*. While the *N. cara* originally described by Agassiz (1865) were relatively small, colonies up to 2–3 inches long, *N. cara* in the NW Atlantic are known to reach much larger sizes: Fewkes (1888) observed colonies up to five feet in length at the entrance to the Bay of Fundy, whereas colonies ranging from 0.2 to 3.7 m were reported to occur in an aggregation observed in the Gulf of Maine by Rogers et al. (1978), the largest ones with 30–40 ectophores and >200 gastrozooids. Sars (1846) observed specimens up to 50 cm long along the Norwegian coast, although we cannot be certain whether these were in fact *N. cara* or *Agalma elegans*. While *N. bijuga* has generally been considered the smaller species, the Pacific colonies from the Gulf of California and Hawaii observed in this study were much larger than their Mediterranean counterparts, having ~30 ectophores each. “Giant colonies” of *Nanomia* have also previously been reported to occur off the west coast of North America (P.R. Pugh, pers. comm. in Mapstone, 2009), and these are likely referring to *N. septata*, which Pugh frequently encountered. Size of the *Nanomia* ectophores also varies, both within and between species (Mapstone, 2009; this study). Variation in the length of the cnidoband and the relative length of the involucrum are also reported by Mapstone (2009). Some of the variation observed in size and morphology may be related to growth and maturation of the colonies, as shown for *N. cara* ectophore morphology.

The genetic division between Atlantic *N. bijuga* and Pacific *N. septata* n.sp. has been previously implied and was not entirely unexpected (Dunn et al., 2005; Park and Lee, 2022). However, our molecular analyses revealed not two, but three or four distinct lineages in addition to the North Atlantic *N. cara*, occurring in (1)

circumglobally in warm waters (*N. bijuga* proper), (2) eastern and western North Pacific (*N. septata* sp. n.), (3) Chinese waters, and (4) Japanese waters. While we here describe *N. septata* sp. n. to represent the molecularly and morphologically distinct north Pacific lineage, we currently lack material to describe the morphological characteristics of the two putative *Nanomia* species recorded from Chinese and Japanese waters. Interestingly, Lo et al. (2013) also reported finding two species of *Nanomia* in waters surrounding Taiwan: One positively identified as *N. bijuga*, and another one that could be assigned to neither *N. bijuga* nor *N. cara*.

The *N. bijuga* proper clade, as delimited by the phylogenetic analyses, also shows geographically structured, hitherto undescribed intraspecific genetic variation (Supplementary Figures S1, S2). This is not surprising, considering the species' circumglobal distribution and likely low gene flow between populations. Resolving the population genetics of *N. bijuga* and concluding whether the morphological characters show consistent regional differences requires further study of multiple specimens from across the geographic range of species.

Our study still lacks data from major oceanic regimes where *Nanomia* are known to occur. Observations attributed to *N. bijuga* have also been recorded from several locations in the Southern Pacific (pers. obs.) and Atlantic, as well as the Indian Ocean and the Red Sea (Alvariño, 1971; Pugh, 1999). Due to the surprising genetic diversity revealed within the genus, further integrated molecular and morphological analyses are necessary to resolve the taxonomy of *Nanomia*, including describing the putative species recorded from Chinese and Japanese waters, as well as to improve our understanding of the biogeography of the genus. Interestingly, our data suggest both intraspecific differentiation of geographically distant populations, as well as adjacent or overlapping species distributions within the genus in both Atlantic and Pacific waters.

The current study employs COI and 16S sequences for the purpose of species delimitation. The observed genetic distances between the species of *Nanomia* resolved by the molecular analyses are relatively large (Table 2), and the 16S data suggest that the genus may in fact not be monophyletic (Figure 3), albeit with low support. However, while good at separating between species, COI and 16S alone are not sufficient for reconstructing phylogenies. Until the remaining *Nanomia* species have been described, and a robust phylogeny including all the putative species has been inferred using a larger set of genetic markers, we refrain from suggesting changes to accepted nomenclature.

5 Conclusion

In this study, we have applied integrated morphological and molecular methods to delimit species in the genus *Nanomia*. We find that *Nanomia septata* sp. n. occurring in the NE Pacific warrants establishment as its own species, based on both molecular and morphological evidence. We provide a first description of *Nanomia septata* sp. n., as well as accounts of the observed *N. bijuga* and *N. cara* material for comparison. We also

observed two additional genetic lineages of *Nanomia* from the West Pacific Ocean, but do not currently have material to examine the morphology of these species to formally describe them. Also lacking are both morphological and molecular data from *Nanomia* from the South Atlantic and regions of the Pacific Ocean, as well as the Indian Ocean, where the genus is also known to occur. Obtaining a comprehensive picture of the diversity of the genus *Nanomia* requires examination of further material from these regions. Nevertheless, the occurrence of several species of *Nanomia* occurring in close proximity to each other raises interesting questions regarding speciation processes in the pelagic realm. Comparable integrated studies on other widespread species and genera are likely to reveal further unexplored diversity within the order Siphonophorae.

Data availability statement

The datasets presented in this study can be found in online repositories. The names of the repository/repositories and accession number(s) can be found in the article/Supplementary Material.

Ethics statement

Ethical approval was not required for the study involving animals in accordance with the local legislation and institutional requirements because study focuses on cnidarian plankton.

Author contributions

AH: Conceptualization, Data curation, Funding acquisition, Investigation, Resources, Visualization, Writing – original draft, Writing – review & editing. LM: Conceptualization, Data curation, Formal analysis, Funding acquisition, Investigation, Resources, Visualization, Writing – original draft, Writing – review & editing. MKM: Conceptualization, Funding acquisition, Investigation, Visualization, Writing – original draft, Writing – review & editing. SHDH: Resources, Visualization, Writing – review & editing. DH: Resources, Visualization, Writing – review & editing. GMM: Conceptualization, Data curation, Investigation, Resources, Visualization, Writing – original draft, Writing – review & editing.

Funding

The author(s) declare financial support was received for the research, authorship, and/or publication of this article. The present study was funded by the Norwegian Biodiversity Information Centre through the Norwegian Taxonomy Initiative projects NorHydro (14-18-70184240) (LM) and HYPNO (48-14-70184233) (AH, LM) in collaboration with the Norwegian Barcode of Life (NorBOL), by grants from the National Science Centre, Poland: 2018/29/N/NZ8/01305 (MKM) and 2019/32/T/

NZ8/00130 (MKM), as well as by Science Foundation Ireland and Marine Harvest Ireland Ltd. (12/RC/2302) (DH) and the Irish Environmental Protection Agency (EPA) (2015-NC-MS-3) (DH). SHDH was supported by the David and Lucile Packard Foundation. The funders were not involved in the study design, collection, analysis, interpretation of data, the writing of this article or the decision to submit it for publication.

Acknowledgments

We wish to thank Dhugal Lindsay, Catriona Munro and Rade Garić for sequences from Japan and the Mediterranean, and morphological specimens from the Adriatic, respectively. Lynne Christianson extracted and sequenced many of the MBARI specimens used in the study. Amy Dozier contributed the original tracing of the nectophore drawings. The help and assistance of the crews of all the vessels involved in the sampling effort are appreciated. David Shale kindly allowed us to use his photos of *Nanomia cara*. The Trustees of the Natural History Museum, London, Canadian Science Publishing, and the Zoological Society of Japan permitted the reproduction of drawings for Figure 1.

References

- Agassiz, A. (1865). "North American Acalephae," in *Illustrated Catalogue of the Museum of Comparative Zoölogy at Harvard College*, vol. 2. (Cambridge (University Press Welch, Bigelow & Co.), Massachusetts), 1–234. doi: 10.5962/bhl.title.1837
- Agassiz, A., and Mayer, A. G. (1902). "Medusæ," in *Report of the scientific research expedition to the tropical Pacific. U.S. Fish Comm. St. Albatross 1899–1900. III.* doi: 10.5962/bhl.title.41325
- Alvarino, A. (1971). Siphonophores of the Pacific with a review of the world distribution. *Bull. Scripps Institution Oceanography* (Cambridge, Massachusetts), 16.
- Bämstedt, U., Fosså, J. H., Martinussen, M. B., and Fosshagen, A. (1998). Mass occurrence of the physonect siphonophore *Apolemia uvaria* (Lesueur) in Norwegian waters. *Sarsia* 83, 79–85. doi: 10.1080/00364827.1998.10413673
- Baxter, E. J., McAllen, R., Allcock, A. L., and Doyle, T. K. (2012). Abundance, distribution and community composition of small gelatinous zooplankton in southern Irish coastal waters. *Biol. Environment: Proc. R. Irish Acad.* 112, 1–13. doi: 10.1353/bae.2012.0029
- Bernston, E. A., France, S. C., and Mullineaux, L. S. (1999). Phylogenetic relationships within the class Anthozoa (phylum Cnidaria) based on nuclear 18S rDNA sequences. *Mol. Phylogenet. Evol.* 13, 417–433. doi: 10.1006/mpev.1999.0649
- Bouillon, J., Medel, M. D., Pagès, F., Gili, J. M., Boero, F., and Gravili, C. (2004). fauna of the mediterranean hydrozoa. *Scientia Marina* 68, 5–449. doi: 10.3989/scimar.2004.68s25
- Browne, E. T., Thompson, I. C., Gamble, F., Herdman, W., Cunningham, J., Beaumont, W., et al. (1898). The fauna and flora of Valencia Harbour on the West Coast of Ireland. *Proc. R. Irish Acad.* 1889–1901) 5, 667–854. Available online at: <https://www.jstor.org/stable/20490564>
- Cartwright, P., Collins, A. G., Dunn, C. W., Evans, N. M., Marques, A. C., Miglietta, M. P., et al. (2008). Phylogenetics of hydrodolina (Hydrozoa: cnidaria). *J. Mar. Biol. Assoc. United Kingdom* 88, 1663–1672. doi: 10.1017/S0025315408002257
- Choy, C. A., Haddock, S. H. D., and Robison, B. H. (2017). Deep pelagic food web structure as revealed by *in situ* feeding observations. *Proc. R. Soc. B: Biol. Sci.* 284, 20172116. doi: 10.1098/rspb.2017.2116
- Church, S. H., Siebert, S., Bhattacharyya, P., and Dunn, C. W. (2015). The histology of *Nanomia bijuga* (Hydrozoa: Siphonophora). *J. Exp. Zoology Part B: Mol. Dev. Evol.* 324, 435–449. doi: 10.1002/jez.b.v324.5
- Cunningham, C. W., and Buss, L. W. (1993). Molecular evidence for multiple episodes of paedomorphism in the family Hydractiniidae. *Biochem. Systematics Ecol.* 21, 57–69. doi: 10.1016/0305-1978(93)90009-G
- Darriba, D., Taboada, G. L., Doallo, R., and Posada, D. (2012). jModelTest 2: more models, new heuristics and parallel computing. *Nat. Methods* 9, 772–772. doi: 10.1038/nmeth.2109
- Delle Chiaje, S. (1841–1844). *Descrizione e notomia degli animali invertebrati della Sicilia citeriore: osservati vivi negli anni 1822–1830 / da S. Delle Chiaje* (Batelli, Naples).
- Dunn, C. W., Pugh, P. R., and Haddock, S. H. D. (2005). Molecular phylogenetics of the siphonophora (Cnidaria), with implications for the evolution of functional specialization. *Systematic Biol.* 54, 916–935. doi: 10.1080/10635150500354837
- Dunn, C. W., and Wagner, G. P. (2006). The evolution of colony-level development in the Siphonophora (Cnidaria: Hydrozoa). *Dev. Genes Evol.* 216, 743–754. doi: 10.1007/s00427-006-0101-8
- Edgar, R. C. (2004). MUSCLE: multiple sequence alignment with high accuracy and high throughput. *Nucleic Acids Res.* 32, 1792–1797. doi: 10.1093/nar/gkh340
- Edwards, M., John, A. W. G., Hunt, H. G., and Lindley, J. A. (1999). Exceptional influx of oceanic species into the North Sea late 1997. *J. Mar. Biol. Assoc. UK* 79, 737–739. doi: 10.1017/S0025315498000885
- Fewkes, J. W. (1888). On certain medusae from New England. *Bull. Museum Comp. Zoology at Harvard Coll.* 13, 209–240.
- Folmer, O., Black, M., Hoeh, W., Lutz, R., and Vrijenhoek, R. (1994). DNA primers for amplification of mitochondrial cytochrome c oxidase subunit I from diverse metazoan invertebrates. *Mol. Mar. Biol. Biotechnol.* 3, 294–299.
- Fosså, J. H., Flood, P. R., Olsen, A. B., and Jensen, F. (2003). Små og usynlige, men plagsomme maneter av arten *Muggiae atlantica*. *Fisken og havet* særnummer 2, 99–103.
- Freeman, G. (1987). Localization of bioluminescence in the siphonophore *Nanomia cara*. *Mar. Biol.* 93, 535–541. doi: 10.1007/BF00392791
- Grossmann, M. M., Collins, A. G., and Lindsay, D. J. (2014). Description of the eudoxid stages of *Lensia havock* and *Lensia leloupi* (Cnidaria: Siphonophora: Calycophorae), with a review of all known *Lensia* eudoxid bracts. *Systematics Biodiversity* 12, 163–180. doi: 10.1080/14772000.2014.902867
- Grossmann, M. M., Lindsay, D. J., and Collins, A. G. (2013). The end of an enigmatic taxon: *Eudoxia macroa* is the eudoxid stage of *Lensia cossack* (Siphonophora, Cnidaria). *Systematics Biodiversity* 11, 381–387. doi: 10.1080/14772000.2013.825658
- Haberlin, D., Mapstone, G., McAllen, R., McEvoy, A. J., and Doyle, T. K. (2016). Diversity and occurrence of siphonophores in Irish coastal waters. *Biol. Environment: Proc. R. Irish Acad.* 116B, 119–129. doi: 10.1353/bae.2016.0016
- Haberlin, D., Raine, R., McAllen, R., and Doyle, T. K. (2019). Distinct gelatinous zooplankton communities across a dynamic shelf sea. *Limnology Oceanography* 64, 1802–1818. doi: 10.1002/lnco.11152
- Hernández-Triana, L. M., Prosser, S. W., Rodríguez-Perez, M. A., Chaverri, L. G., Hebert, P. D., and Gregory, T. R. (2014). Recovery of DNA barcodes from blackfly

Conflict of interest

The authors declare that the research was conducted in the absence of any commercial or financial relationships that could be construed as a potential conflict of interest.

Publisher's note

All claims expressed in this article are solely those of the authors and do not necessarily represent those of their affiliated organizations, or those of the publisher, the editors and the reviewers. Any product that may be evaluated in this article, or claim that may be made by its manufacturer, is not guaranteed or endorsed by the publisher.

Supplementary material

The Supplementary Material for this article can be found online at: <https://www.frontiersin.org/articles/10.3389/fmars.2024.1421514/full#supplementary-material>

- museum specimens (Diptera: Simuliidae) using primer sets that target a variety of sequence lengths. *Mol. Ecol. Resour.* 14, 508–518. doi: 10.1111/1755-0998.12208
- Hosia, A., and Båmstedt, U. (2008). Seasonal abundance and vertical distribution of siphonophores in western Norwegian fjords. *J. Plankton Res.* 30, 951–962. doi: 10.1093/plankt/fbn045
- Johnson, S. B., Winnikoff, J. R., Schultz, D. T., Christianson, L. M., Patry, W. L., Mills, C. E., et al. (2022). Speciation of pelagic zooplankton: Invisible boundaries can drive isolation of oceanic ctenophores. *Front. Genet.* 13. doi: 10.3389/fgene.2022.970314
- Kawamura, T. (1911). “Shidarezakura Kurage” and “Nagayoraku Kurage” *Cupulita picta* Metschnikoff and *Agalmopsis elegans* Sars. *Dobutz Z Tokyo* 23, 359–363.
- Kearse, M., Moir, R., Wilson, A., Stones-Havas, S., Cheung, M., Sturrock, S., et al. (2012). Geneious Basic: an integrated and extendable desktop software platform for the organization and analysis of sequence data. *Bioinformatics* 28, 1647–1649. doi: 10.1093/bioinformatics/bts199
- Kirkpatrick, P. A., and Pugh, P. R. (1984). Siphonophores and velellids. *Synopsis Br. Fauna (New Series)* 29, 1–154. doi: 10.1163/9789004627550
- Knutsen, T., Hosia, A., Falkenhaug, T., Skern-Mauritzen, R., Wiebe, P. H., Larsen, R. B., et al. (2018). Coincident mass occurrence of gelatinous zooplankton in northern norway. *Front. Mar. Sci.* 5. doi: 10.3389/fmars.2018.00158
- Kumar, S., Stecher, G., Li, M., Knyaz, C., and Tamura, K. (2018). MEGA X: Molecular evolutionary genetics analysis across computing platforms. *Mol. Biol. Evol.* 35, 1547–1549. doi: 10.1093/molbev/msy096
- Lindsay, D. J., Grossmann, M. M., and Nishikawa, J. U. N. (2015). DNA barcoding of pelagic cnidarians: current status and future prospects. *Bull. Plankton Soc. Japan* 62, 39–43. doi: 10.24763/bpsj.62.1_39
- Lo, W.-T., Yu, S.-F., and Hsieh, H.-Y. (2013). Effects of summer mesoscale hydrographic features on epipelagic siphonophore assemblages in the surrounding waters of Taiwan, western North Pacific Ocean. *J. Oceanography* 69, 495–509. doi: 10.1007/s10872-013-0188-2
- Mackie, G. O. (1963). “Siphonophores, bud-colonies and superorganisms,” in *The Lower Metazoa; Comparative Biology and Phylogeny*. Ed. E. Dougherty (University of California Press, Berkeley), 329–337.
- Mackie, G. O. (1964). Analysis of locomotion in a siphonophore colony. *Proc. R. Soc. London Ser. B Biol. Sci.* 159, 366–391. doi: 10.1098/rspb.1964.0008
- Mackie, G. O. (1986). From aggregates to integrates: physiological aspects of modularity in colonial animals. *Philos. Trans. R. Soc. London B Biol. Sci.* 313, 175–196. doi: 10.1098/rstb.1986.0032
- Mackie, G. O. (2002). What's new in cnidarian biology? *Can. J. Zool.* 80 (10), 1649–1653. doi: 10.1139/z02-138
- Mapstone, G. M. (2009). *Siphonophora (Cnidaria, hydrozoa) of canadian pacific waters* (Ottawa: NRC Research Press), 302.
- Mapstone, G. M. (2014). Global diversity and review of Siphonophorae (Cnidaria: Hydrozoa). *PLoS One* 9, e87737. doi: 10.1371/journal.pone.0087737
- Mapstone, G. M., and Arai, M. N. (1992). “Abundance and vertical distribution of Siphonophores (Cnidaria) from the Central Strait of Georgia, British Columbia, during spring and summer,” in *Contributions to Natural Science*, vol. 15. (Royal British Columbia Museum, Victoria).
- Mills, C. E. (1995). Medusae, siphonophores, and ctenophores as planktivorous predators in changing global ecosystems. *ICES J. Mar. Sci.* 52, 575–581. doi: 10.1016/1054-3139(95)80072-7
- Munro, C., Siebert, S., Zapata, F., Howison, M., Damian-Serrano, A., Church, S. H., et al. (2018). Improved phylogenetic resolution within Siphonophora (Cnidaria) with implications for trait evolution. *Mol. Phylogenet. Evol.* 127, 823–833. doi: 10.1016/j.ympev.2018.06.030
- Norekian, T. P., and Meech, R. W. (2020). Structure and function of the nervous system in nectophores of the siphonophore *Nanomia bijuga*. *J. Exp. Biol.* 223, jeb233494. doi: 10.1242/jeb.233494
- Norris, R. D. (2000). Pelagic species diversity, biogeography, and evolution. *Paleobiology* 26, 236–258. doi: 10.1666/0094-8373(2000)26[236:PSDBAE]2.0.CO;2
- Ortman, B. D., Bucklin, A., Pages, F., and Youngbluth, M. (2010). DNA barcoding the Medusozoa using mtCOI. *Deep-Sea Res. Part II-Topical Stud. Oceanography* 57, 2148–2156. doi: 10.1016/j.dsr2.2010.09.017
- Pagès, F., and Gili, J.-M. (1992). Medusae (Hydrozoa, scyphozoa, cubozoa) of the Benguela current (southeastern Atlantic). *Scientia Marina* 56, 1–64.
- Panasuk, A., Jaźdewska, A., Slomska, A., Irzycka, M., and Wawrzynek, J. (2019). Genetic identity of two physonect siphonophores from Southern Ocean waters – the enigmatic taxon *Mica micula* and *Pyrostephos vanhoefeni*. *J. Mar. Biol. Assoc. United Kingdom* 99, 303–310. doi: 10.1017/S0025315418000218
- Park, N., and Lee, W. (2022). Eight new records of Siphonophores (Cnidaria: Hydrozoa) in Korean waters. *Diversity* 4, 494. doi: 10.3390/d14060494
- Pontin, D. R., and Cruickshank, R. H. (2012). Molecular phylogenetics of the genus *Physalia* (Cnidaria: Siphonophora) in New Zealand coastal waters reveals cryptic diversity. *Hydrobiologia* 686, 91–105. doi: 10.1007/s10750-011-0994-8
- Pugh, P. R. (1999). “Siphonophorae,” in *South Atlantic Zooplankton*, vol. 1. Ed. D. Boltovskoy (Backhuys Publishers, Leiden), 467–511, ISBN: .
- Puillandre, N., Brouillet, S., and Achaz, G. (2021). ASAP: assemble species by automatic partitioning. *Mol. Ecol. Resour.* 21, 609–620. doi: 10.1111/1755-0998.13281
- Quoy, J. R. C., and Gaimard, J. P. (1824). Voyage autour du monde, entrepris par ordre du roi. Exécuté sur les corvettes de S.M. l'Uranie et la Physicienne, pendant les années 1817, 1818, 1819 et 1820. *Zoologie. Parte 2 et Atlas.* (Chez Pillat, Paris). doi: 10.5962/bhl.title.152367
- Rogers, C. A., Biggs, D. C., and Cooper, R. A. (1978). Aggregations of the siphonophore *Nanomia cara* in the Gulf of Maine: Observations from a submersible. *Fishery Bull.* 76, 281–284.
- Ronquist, F., Teslenko, M., van der Mark, P., Ayres, D. L., Darling, A., Höhna, S., et al. (2012). MrBayes 3.2: efficient Bayesian phylogenetic inference and model choice across a large model space. *Syst. Biol.* 61, 539–542. doi: 10.1093/sysbio/sys029
- Sars, M. (1846). *Fauna Littoralis Norvegiae* Vol. 1 (Johann Dahl, Christiania).
- Schuchert, P. (2024). World Hydrozoa Database. Available online at: <https://www.marinespecies.org/hydrozoa>. (Accessed September 29, 2024).
- Siebert, S., Goetz, F. E., Church, S. H., Bhattacharyya, P., Zapata, F., Haddock, S. H., et al. (2015). Stem cells in *Nanomia bijuga* (Siphonophora), a colonial animal with localized growth zones. *EvoDevo* 6, 22. doi: 10.1186/s13227-015-0018-2
- Siebert, S., Robinson, M. D., Tintori, S. C., Goetz, F., Helm, R. R., Smith, S. A., et al. (2011). Differential gene expression in the siphonophore *Nanomia bijuga* (Cnidaria) assessed with multiple next-generation sequencing workflows. *PLoS One* 6, e22953. doi: 10.1371/journal.pone.0022953
- Spencer, A. N. (1971). Myoid conduction in the siphonophore *Nanomia bijuga*. *Nature* 233, 490–491. doi: 10.1038/233490a0
- Stamatakis, A. (2014). RAxML version 8: a tool for phylogenetic analysis and post-analysis of large phylogenies. *Bioinformatics* 30, 1312–1313. doi: 10.1093/bioinformatics/btu033
- Sutherland, K. R., Gemmell, B. J., Colin, S. P., and Costello, J. H. (2019). Maneuvering performance in the colonial siphonophore, *Nanomia bijuga*. *Biomimetics* 4, 62. doi: 10.3390/biomimetics4030062
- Totton, A. K. (1954). Siphonophora of the Indian Ocean together with systematic and biological notes on related specimens from other oceans. *Discovery Rep.* 27, 1–162.
- Totton, A. K. (1965). *A synopsis of the Siphonophora* (London: Trustees of the British Museum (Natural History)).
- Zhang, J., Kapli, P., Pavlidis, P., and Stamatakis, A. (2013). A general species delimitation method with applications to phylogenetic placements. *Bioinformatics* 29, 2869–2876. doi: 10.1093/bioinformatics/btt499
- Zheng, L., He, J., Lin, Y., Cao, W., and Zhang, W. (2014). 16S rRNA is a better choice than COI for DNA barcoding hydrozoans in the coastal waters of China. *Acta Oceanologica Sin.* 33, 55–76. doi: 10.1007/s13131-014-0415-8